

Answer to the editor and reviewers

We thank the editor and the two reviewers for their constructive comments. We reply to all the comments point by point below. We have also included a new version of the manuscript with the modifications highlighted in red at the end.

1 Answer to Reviewer 1

R1: *This paper describes simulation experiments with the CLIMBER-2 EMIC model in order to understand carbon cycle dynamics over Termination I. Here, simulation results are compared with atmospheric CO₂, atmospheric ¹³CO₂, and deep ocean δ¹³C in the Southern Ocean evolving over time between 20 and 10 kyr BP. In principle this is still a topic not finally understood and therefore a welcome contribution well fitted within the scope of the journal.*

1 General appearance

R1: *In general terms the papers is written in a way which is very often not exact in the details and therefore the written text needs a major improvement. This manifests for example in the way how changes over time are described. The authors try to simulate forward in time the changes in the carbon cycle, thus they evolve their model from LGM to the beginning of the Holocene implying a rise in CO₂ over time. However, very often this is confused with a decrease in CO₂, which is correct in absolute terms with respect to today, but which is in the context of forward modelling not correct. Which makes things very difficult is that it is not consistently wrong, but mixed up. Further below I list examples which should be revised accordingly.*

Answer: To avoid confusion we speak only of CO₂ increase when discussing the transient simulations, and when discussing the initial equilibrium glacial state we have replaced the “drawdown”, “drop”... terms by “change” and/or added some precision on the fact that it was relative to the Pre-industrial level.

R1: *This was about wording and readability. Other points for improvements concern rather vague explanations in the way how changes are described. For example, in the introduction it is said that the glacial state was -2 to -6° C colder in the Southern Ocean. But what variable is meant here? SST? Deep ocean temperature? Surface air temperature?*

Answer: It is the sea surface temperature. It has been added in the text: “sea surface temperature of -2 to -6°C cooler relative to today in the Southern Ocean”

R1: *Another example: It is often written about the “increase of the terrestrial biosphere”. The is no such thing, it probably means that the C content of the terrestrial biosphere increases, but this should then also be written down. Unfortunately, this consists throughout the MS and need a major improvement to get the article in an acceptable shape.*

Answer: As suggested, when the changes relate to the carbon content of the terrestrial biosphere, we have added “carbon content” to it. It is thus now the “terrestrial biosphere carbon content” which increases or decreases.

2. Major suggestions concerning the content

1. Other papers

R1: *The novel aspect of this study is the use of an EMIC transient over time with an interactive carbon cycle. Similar experiments so far were focusing on box modeling approaches. However, the authors are not addressing two recent studies under discussion in this same journal, which are:*

- *Deep ocean ventilation, carbon isotopes, marine sedimentation and the deglacial CO₂ rise T. Tschumi, F. Joos, M. Gehlen, and C. Heinze Clim. Past Discuss., 6, 1895-1958, 2010*
- *Glacial CO₂ cycle as a succession of key physical and biogeochemical processes V. Brovkin, A. Ganopolski, D. Archer, and G. Munhoven Clim. Past Discuss., 7, 1767-1795, 2011*

While the Tschumi paper seemed to be very likely published in a revised version (according to the online discussion), not a lot can be said about the status of the Brovkin paper, however as there the same model is used - CLIMBER- 2, I think the approaches of both papers should be discussed widely within the present paper. While the Tschumi paper analyses the impact of different processes on the carbon cycle starting from a constant climate (comparable to sect 3.1 of the Bouttes paper), Brovkin simulates a full glacial cycle (120 kyr). Both papers make strong cases about how their approaches can explain some fraction of data-based changes over the glacial/interglacial cycles without the apparent major process of the Bouttes approach (brine rejection). This should be discussed as wide and as far as possible. I acknowledge, that both papers are not finally published, but since they are discussed already the authors should address how their findings can be compared with them. Discussion papers available online here opens for the possibility to include comparing discussions of papers on the same subject much earlier than when submitted to more classical journals without this open discussion section. This should be seen as opportunity to speed up the scientific discussion.

Answer: As suggested by the reviewer we have added a discussion of the two papers in the manuscript.

"Recently, two papers studied the evolution of the carbon cycle in the context of glacial-interglacial cycles. Tschumi et al. (2011) run transient simulations testing the sensitivity of various mechanisms in a constant climate. The simulations support the hypothesis that a change in the ventilation of the deep ocean played an important role in the variation of CO₂ during glacial interglacial cycles. In this study, the change of deep ocean ventilation was obtained by changing the windstress whereas in our study the change of deep ocean stratification results from changing the sinking of brines. Our study also supports the important role of the change of deep ocean stratification. Furthermore it demonstrates that it allows to simulate the evolution of CO₂ during the last deglaciation in agreement with CO₂ and $\delta^{13}\text{C}$ data without prescribing CO₂. In particular, the interactive carbon-climate simulation manages to capture not only the right CO₂ amplitude change, but also the right timing. With other mechanisms, Brovkin et al. (2011) run a full glacial-interglacial evolution of CO₂ and northern ice sheets. In this simulation the role of the carbonate compensation due to changes in the weathering rate is important. However, although most of the CO₂ evolution is successfully simulated, the timing of the CO₂ rise during the deglaciation lags the data indicating that a mechanism leading to an earlier CO₂ change is missing. With the change of deep stratification from the change of sinking of brines it allows us to get this timing right, although it relies on scenarios that need to be confirmed."

2. Forcings

R1: *The authors claim, that they for the first time have an EMIC simulation forward in time with an interactive C cycle. They state insolation, ice sheet extent and atmospheric CO₂ content as only forcing of the model. If the CO₂ is now calculated interactively it implies that for those results that do not meet the measured values the forcing would be smaller than for those scenarios where CO₂ perfectly matches the data. This would have feedback effects, e.g. small change in CO₂ leads*

to smaller change in global temperature, which again leads to a smaller CO_2 change in the ocean carbon uptake/release (via solubility pump) or C storage on land. To give the reader a possibility to estimate how large these feedback effects might be, it is desirable to have the relative size of the forcing explained, e.g. insolation, ice sheet, CO_2 .

Answer: As highlighted by the reviewer, the CO_2 predicted by the model can be very different from the one imposed. This results in a carbon-climate feedback and the model equilibrates at a different state (Figure 13). The amplitude of each forcing would not give important insights on the feedbacks as the system has an important inertia and as figure 13 shows it takes at least 10000 years to equilibrate. Knowing the initial relative sizes of the forcings will thus not be informative on the differences when the system equilibrates.

In the manuscript we have modified section 3.3.1 as follows: “In the “LGM-ctrl” run, CO_2 increases from ~ 254 ppm and equilibrates close to preindustrial level (~ 284 ppm) (Figure 13). The atmospheric CO_2 level is higher than the CO_2 prescribed due to the carbon-climate feedbacks. Indeed, higher CO_2 leads to higher temperature, which mainly reduces ocean solubility and further increases atmospheric CO_2 until it equilibrates.”

R1: *Furthermore, what about the radiative forcing of other two greenhouse gases CH_4 and N_2O which contribute to a forcing which is about 30% of that of CO_2 ?*

Answer: As done previously, CH_4 and N_2O are not explicitly considered in the model, but the CO_2 is an “equivalent CO_2 ” that considers the change of CH_4 and N_2O (Brovkin et al., 2007). This precision has been added in the text in the method section: “ CH_4 and N_2O are not explicitly considered in the model, but the CO_2 is an “equivalent CO_2 ” that considers the change of CH_4 and N_2O (Brovkin et al., 2007).”

3. Temperature: initial distribution and evolution, and stratification change

R1: *I acknowledge that the C cycle is in focus here. But to set the overall model performance into context to data it should be shown, how temperature evolves over time. It should briefly be expanded on the climate state at the end of the initialisation (after 50 000 yr) to see the general performance of the model. This is in detail probably written in other papers, but to make this paper here more independent especially the distribution of temperature should be analysed. Is the model in a similar state than in a previous application, analysing an LGM to be -5.8 K cooling than preindustrial times (Schneider von Deimling et al., 2006)?*

Answer: We have added a brief description of the temperature change in the glacial simulation compared to the preindustrial at the beginning and for the interactive simulation:

“At the end of the 50,000 year simulation, the global mean air temperature with the preindustrial boundary conditions is $12.9^\circ C$. With the LGM conditions, the climate is $3.3^\circ C$ colder. The effect of the dust is not taken into account in this study. According to von Deimling et al. (2006), it would cool the global climate by an additional $1.35 \pm 0.35^\circ C$, yielding an approximately $4.65 \pm 0.35^\circ C$ colder climate during the LGM compared to the preindustrial. It is in the lower range of the estimation from von Deimling et al. (2006), but the corresponding sea surface temperature change, which is $-2^\circ C$ for the LGM, is in good agreement with the MARGO database ($-1.9^\circ C$).”

“With these three additional mechanisms (“LGM-all”), the climate at the end of the 50,000 year simulation is slightly colder compared to the standard glacial simulation ($0.3^\circ C$ colder). The global air temperature during the LGM is $3.6^\circ C$ colder compared to the preindustrial and the corresponding SST change is $2.3^\circ C$.”

R1: *Furthermore, how is temperature evolving over time in the interactive final run?*

Answer: We have added a figure of the evolution of the temperature in the interactive final runs (figure 16) and a discussion: “Although the amplitude of the glacial-interglacial Antarctic temperature change is underestimated in the model, it is possible to analyse the relative timing of CO₂ and temperature evolution (Figure 16). The two scenarios that agree best with CO₂ and $\delta^{13}\text{C}$ data (“abrupt 17k” and “intermediate”) result in a lead of temperature relative to CO₂ as inferred from termination 3 data (Caillon et al., 2003). The halt of the sinking of brines not only breaks down the stratification, which increases CO₂ and therefore temperature, but also induces a decrease in sea ice formation (which is computed by a thermodynamic sea ice model) as the surface waters become saltier and warmer. Such an early deglacial retreat of sea ice is also indicated in the data (Shemesh et al., 2002). Because of the reduced albedo, temperature then increases, resulting in a positive feedback. Antarctic temperature thus reacts quicker than CO₂ at the beginning of the termination, despite the same unique triggering, i.e. the halt of stratification due to brines sinking.”

R1: *As the only non-C cycle aspect the change in ocean circulation were plotted in Fig 5 and 12. However, they are hardly explained in the text, which should be expanded.*

Answer: Following the reviewer’s advice we have added a discussion on the change of ocean circulation:

“Indeed, with the stratification induced by the sinking of brines the maximum of the NADW export is around 15 Sv compared to around 20 Sv without it. When the stratification breaks down the formation of deep water intensifies rapidly to 22 Sv in around 1500 years. It then decreases more slowly back to 20 Sv.”

“The maximum export of NADW increases gradually from 15 Sv to around 20 Sv, the latter being reached after around 4500 years (Figure 5).”

“After a first rapid increase similar to the one without the interactive diffusion (it reaches 20 Sv after around 500 years), the maximum export of NADW very slowly increases of around 1 Sv in around 3500 years (Figure 5). As the stratification breaks down the diffusion coefficient, which is interactively computed, increases as well. Because the mixing increases it tends to diminish the density gradient and the export of water. As a consequence it leads to the same delay in the carbon evolution.”

R1: *Furthermore, if the stratification is changed in the Southern Ocean by the brine process, it would be good to see HOW stratification is changed. Or should that be seen as AABW in Figs 5 and 12?*

Answer: We have added a figure showing the evolution of the DIC and density during the interactive simulation (figure 15).

4. Combination of the three mechanisms

R1: *In their ultimate last scenario the authors calculate with interactive C cycle and include all the three processes introduces before, which are iron fertilisation, brine rejection and a stratification-dependent diffusion (sect 3.3). However, in all previous investigations (sec 3.1 and 3.2) without interactive C cycle all three were never used together, they were either analysed individually or in pairwise combinations (brine+iron, brine+diffusion). This is most confusing. If the combination of all three processes are the ultimate suggestions of this papers to explain the data this should also be investigated without interactive C cycle coupling and from steady state climate.*

Answer: With the three additional mechanisms the evolution of CO₂ is close to the data, hence the results obtained with the interactive simulations are close to the ones with the simulation forced by the CO₂ from the data (Additionnal Figure below). Adding these results would thus make the

manuscript longer without bringing really new insights.

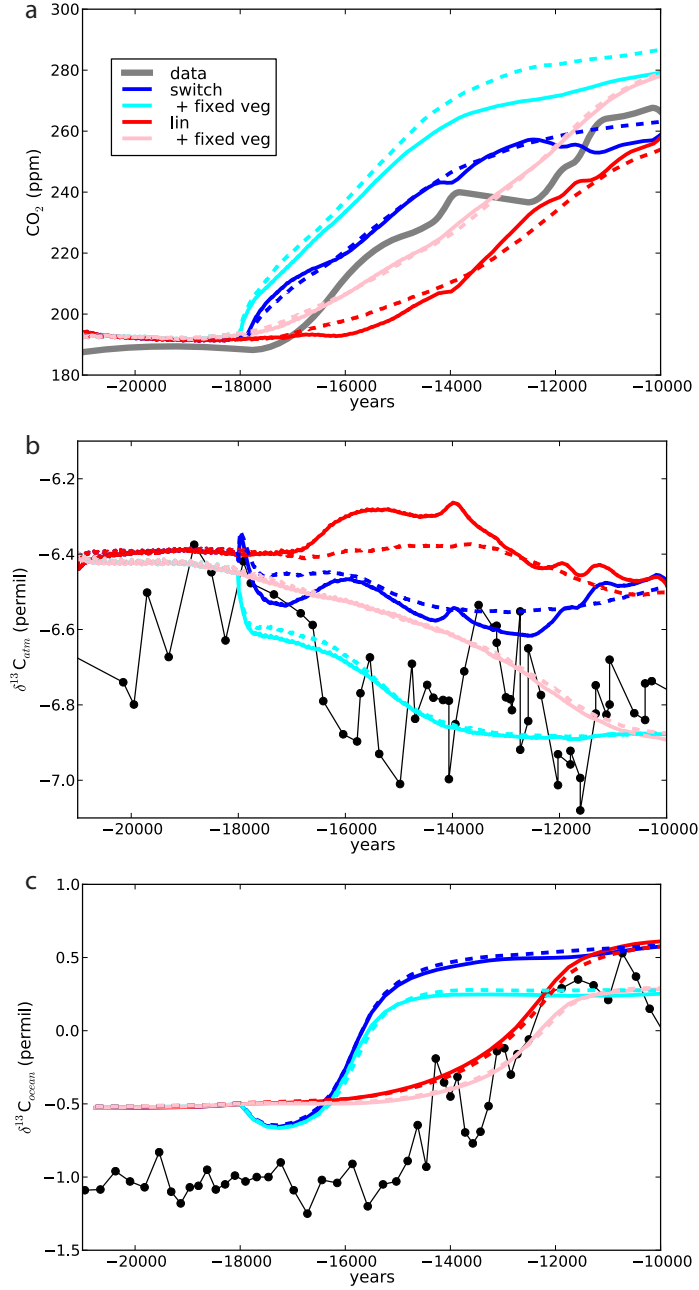


Figure 1: Additional figure: evolution of CO₂, oceanic δ¹³C and atmospheric δ¹³C for the “switch” and “linear” scenarios. The solid lines represent the simulations with prescribed CO₂ and the dotted lines the simulations with interactive CO₂, which are generally similar.

5. Age models of the data used

R1: : As the authors try to make statements for transient simulations including the comparison

with proxy data some more care is necessary concerning the dating of the different data sets. The authors show ice core CO_2 data from two studies (Monnin, Laurantou). However in both study different age models are used for presentation of the data which leads to an offset in the start of the CO_2 rise by some centuries. This might in detail not be resolvable in the simulation results, but for comparison and completeness the used age model should be stated. Similarly, the iron fertilisation is said to follow dust transport according Wolff et al. (2006). In this paper ice core data from EPICA Dome C are plotted on an older age model, EDC2, while things look slightly different on the new age model EDC3 (Parrenin et al., 2007). Thus, for completeness it first needs to be known which age model is used, and second it should at best be the same (and probably the most recent) one as the one used for the CO_2 and $\delta^{13}C$ record. Additionally, why do the authors say they synchronise iron fertilisation to dust transport, when in the Wolff paper iron fluxes (not only dust fluxes) itself are given. This should be revised accordingly.

Answer: The CO_2 data that we use from Laurantou and Monnin are both on the EDC3 age model, so there is no offset for CO_2 . For iron fertilization we have used the iron flux and not the dust flux as previously written in the text, which we have modified. The Fe flux is however on the EDC2 age model. It would be better to have it on the EDC3 age model, but in this study we look at the general trend and the offset is under the resolution of interest and thus does not change the result.

6. Evolution of brines

R1: : *Going in the same direction, the way how the brine scenario is forced (changes in the respective parameter “frac” starting at 18 kyr BP either abrupt or linearly) is only weakly motivated. In explaining the brine process in Fig. 7 I had the impression the maximum brine rejection should be during the termination with smaller values during LGM and during interglacials. This is not the case, brine is only reduced from LGM values. Furthermore the timing seemed to be arbitrary. Thus some more statements if and how this process might be coupled to sea level evolution are wanted and might in the end lead to a different timing!*

Answer: The evolution of the sinking of brines would depend on the volume of water above the ice shelves. It should thus depend on two parameters: the sea level change (which primarily depends on the evolution of the Northern Ice Sheets) and the advance and retreat of the Antarctic ice sheet. Although the evolution of sea level can be constrained by proxy data, the evolution of the Antarctic ice sheet on the shelves is not very well constrained yet. In this study we thus test different scenarios, but future work would benefit from taking advantage of simulations of the advance and retreat of the Antarctic ice sheet during the deglaciation. We have expanded the discussion on that topic in the manuscript:

“The halt of the sinking of brines imposed in the model would in reality be due to the change of topography around Antarctica (Figure 7). **Indeed, the sinking of brines would depend on the volume of water above the shelves. It would thus depend on two variables: the evolution of sea level and the advance/retreat of the Antarctic ice sheet on the shelves.** During interglacials, the volume of water above the continental shelves is important and some mixing of the salt rejected by sea ice formation happens. The salty dense water can thus not easily sink to the bottom of the ocean (Figure 7a). During the glaciation, the Antarctic ice sheet progressively increases both in volume and extension (Figure 7b). Because of the extension of the ice sheet and the sea level fall, the volume of water above the Antarctic ice shelves is reduced and the salt less diluted. Moreover, the release of salt increases as more sea ice is formed (in particular as the seasonality seems to increase (Gersonde et al., 2005)). The salt rejected by sea ice formation can accumulate more and create very dense water susceptible to flow more easily down to the abyss. This is modelled by an increase of the fraction of salt that sinks to the deep ocean, the *frac* parameter. When the ice sheet reaches its maximum extent, i.e.

when the continental shelves are covered, a few thousand years after the Last Glacial Maximum (Ritz et al., 2001; Huybrechts, 2002), the sea ice formation is shifted to the open ocean. The absence of shelf where the brines sink, accumulate and create very dense water susceptible to flow down to the abyss, prevents the deep sinking of brines (Figure 7c). **In the open ocean, the dilution of the brines released by sea ice is more important and the effect of the brine-generated dense water disappears.** If the continental shelves are **all** covered simultaneously it results in an abrupt halt of the sinking of brines. Alternatively, the halt of the sinking of brines can be linked to the sea level rise, which increases the volume of water above the continental shelf leading to more mixing and less sinking of dense water. It corresponds to a more progressive reduction of the sinking of brines, which can be first approximated by a linear decrease. These two extreme scenarios (“linear” and “abrupt”) of the halt of the sinking of brines are both tested. The two scenarios explore the two extreme cases, a more probable one would lie between the two. **Because the glaciation and deglaciation are not symmetrical with respect to the sea level change and advance and retreat of Antarctica on the ice shelves, the evolution of the sinking of brines would also not be symmetrical. In particular, according to data, the Antarctic ice sheet melting starts later than the northern ones, around 14 kyr BP (Clark et al., 2009; Mackintosh et al., 2011). At that time, the already higher sea level (due to the melting of the Northern ice sheets that started earlier) associated to the input of fresh water from the melting of the Antarctic ice sheet can then prevent important sinking of brines to happen again. It is thus not possible to exclude that some sinking of the brines occurred again (although not at the very beginning of the deglaciation since it was inhibited by the presence of the Antarctic ice sheet on the shelves), yet it would be relatively less important. However, this possibility is beyond the scope of this study, which explores the mean trend during the deglaciation, and would require further work to focus on the effect of a brief activation of the sinking of brines during the deglaciation, probably in link with more rapid events.”**

7. $\delta^{13}C$

R1: *It was chosen to simulate the last glacial/interglacial transition without abrupt climate changes connected with the Heinrich 1 event and the Younger Dryas. It is therefore a priori clear that the dynamics contained in the atmospheric $\delta^{13}CO_2$ record can not be matched. As written at least twice throughout the text the $\delta^{13}CO_2$ record of Lourantou contains a w-shape. Lourantou et al. already provided a lot of evidences that this might be caused by the rapid climate changes during Termination I. To streamline the whole paper the authors might consider to drop the whole discussion of the $\delta^{13}CO_2$ record. This might especially be important when the discussion and results sections are extended as suggested here.*

Answer: The evolution of atmospheric $\delta^{13}C$ brings additional constraints. The W-shape, which is not well simulated by the model, shows that abrupt events are likely to play a role. However, the simulations nonetheless bring new insights to the fact that the vegetation evolution has an impact equally important as the one from the ocean, which was only tested with box models in Lourantou et al. (2008). Moreover, the general evolution is better simulated when the vegetation is fixed, and the W-shape could be simulated if the vegetation would increase then decrease during the deglaciation. It thus adds further motivation for further work focusing on the evolution of the vegetation during the deglaciation and its impact on $\delta^{13}CO_2$. We have modified one of the sentences as follows:

“It confirms that the evolution of the terrestrial biosphere has an important impact on $\delta^{13}C_{atm}$ (?) and should be studied in more details in the future.”

8. Factorial analysis

R1: *The paper misses a final analysis in which the contribution of various processes over time*

are disentangled. The authors finally agree on a best guess scenario, but how much of the changes in ocean $\delta^{13}\text{C}$ and atmospheric CO_2 is due to a) the physics (solubility pump (changes in SST), ocean circulation (including the brine and diffusion mechanism), b) biological pump (iron fertilisation, but also changes in marine biota due to changes in climate), c) terrestrial C uptake. I realised this kind of fractional analysis was presented for LGM steady state in Bouttes et al. 2011 GRL, Fig.3. So the authors might consider if this figure might be extended towards a time-dependent version. One might then learn, which processes change first and initiate the whole changes in the C cycle.

Answer: It seems complicated to do a time-dependent version of the GRL study. Nonetheless, in our scenario the most important processes arise from the dynamics. The change of stratification due to the sinking of brines is the predominant mechanism at work.

3 Minors in chronological order

R1: 1. Intro and results: Evolution of the depth gradient in $\delta^{13}\text{C}$ in the Southern Ocean is published in Hodell et al. (2003).

Answer: As suggested, we have added the reference in the introduction.

R1: 2. Intro, 2nd paragraph page 1890: Here, the thinking in temporal evolution of processes and in changes from present day is mixed up. They write about a “ CO_2 increase” (thus thinking in the evolution of CO_2 , not in the change from present days). But CO_2 INCREASES due to a reduced (not enhanced) biological pump, CO_2 should rise (not drop), sea ice over Termination I is reduced (not increased). It is impossible to list all confusing statements here, thus this is illustrative to make the authors aware how they mix up both ways of describing the changes. A careful revision of the whole text for these things is necessary.

Answer: The description of mechanisms as work during glacial periods compared to to interglacial and during the deglaciation was indeed not clear enough; we have changed it to avoid mixing as shown in the following: “Enhanced marine biology by iron fertilization **during glacial period, which would then decrease during the deglaciation**, is assumed to play a role (Martin, 1990), although of relatively small importance as it could account for a 15-20 ppm **change** (i.e. approximately 20 % of the ~ 90 ppm total **CO_2 change**) (Bopp et al., 2003; Tagliabue et al., 2009). Carbonate compensation is a recognized process that amplifies the uptake **or loss** of carbon by the ocean (Broecker and Peng, 1987; Archer et al., 2000; Brovkin et al., 2007). Finally, changes in the oceanic circulation and mixing can have a significant impact on glacial CO_2 (Toggweiler, 1999; Paillard and Parrenin, 2004; Köhler et al., 2005; Watson and Garabato, 2005; Bouttes et al., 2009; Skinner et al., 2010). In particular, it has been recently shown that the deep stratification induced by enhanced brine sinking can strongly decrease CO_2 during the LGM **relative to the Pre-industrial** and simultaneously increase the upper to deep **ocean $\delta^{13}\text{C}$** gradient, in line with data (Bouttes et al., 2010, 2011).”

R1: 3. Section 2.2.1: Proxy-based evidences of a changed biological pump highly depend on the location, e.g. north or south of the polar front, see Kohfeld et al. (2005). Is this relevant here?

Answer: Yes, according to Kohfeld et al., 2005, there was an increase of productivity during the LGM north of the modern day Antarctic polar front, but none south of it. We have added the following in the manuscript: “According to proxy-based study of the change of productivity this effect would have been restrained to the areas north of the modern-day Antarctic polar front (Kohfeld et al., 2005).”

R1: 4. Section 2.2.2 and 2.2.3: In explaining your scenarios your should also mention, which is

the chosen parameter value used here for frac and α and how the chosen value refer to the previous studies (2011 in GRL), e.g. were they taken as the best guess from previous simulations, or were they fitted / tuned especially for the dynamics during Termination I investigated here?

Answer: We have added some details about the values of the two parameters: first there are set to their maximum potential value, then in the last experiment with the three mechanisms we use a set of values taken from Bouttes et al. (2011).

“This is a simple parameterization of the effect of iron fertilization as the iron cycle is not simulated in the model. As done in Bouttes et al. (2011), we use a parameter to vary this effect between 0 and 1. This parameter is first set to 1 to explore the maximum potential effect of this mechanism. In the last section we use a combination of the three mechanisms from Bouttes et al. (2011) in which this parameter is set to 0.3. ”

“A previous study exploring its role during the LGM has shown that it could vary between 0.7 and 0.9 (Bouttes et al., 2011). **We first use the maximum value of 0.9 to test the maximum impact of this mechanism. In the last section we use a combination of the three mechanisms from Bouttes et al. (2011) where $\alpha=0.7$.** ”

R1: 5. *Results for constant climate (sect 3.1): I think the way you calculate the return to near equilibrium by reaching 95% of the equilibrium values is maybe too simplistic. For CO_2 95% of the equilibrium value of about 257 ppm is 244 ppmv (-13 ppm). The CO_2 anomaly in the iron fertilisation scenario is only 29 ppm. Thus by a rise of only $29-13 = 16$ ppm this equilibrium threshold is crossed. Furthermore it lead to an analysis where the equilibrium is already achieved, while changes are already underway, e.g. in the linear scenarios of IRON or BRINES (equilibrium reached after 4400 yr, but changes is for 5000 yr). I therefore suggest to choose an even stricter threshold (e.g. 99%) or you define the reach of equilibrium with respect to the CO_2 anomaly. E.g. in IRON CO_2 initially is reduced by 29 ppm, so calculate until 95% from this anomaly is again gained back, thus when CO_2 rises by 27.6 ppm after the start of the change in the forcing.*

Answer: As highlighted by the reviewer the description of the way we calculate the return to near equilibrium is not exact as it is in fact the second way suggested by the reviewer, i.e. we calculate when the change is 95% of the anomaly. We have thus changed this description in the manuscript: “To compare the time needed by the system to reach a near-equilibrium state we consider the time when the anomaly of a considered variable (defined as the difference between its value and its initial value) has reached 95% of the anomaly of the equilibrium state (Table 2).”

And the caption of Table 2: “Time for the anomaly of the considered variable (defined as the difference between its value and the initial value) to reach 95% of the equilibrium anomaly value (equilibrium anomaly value taken as the difference between the value at year 12000 of the simulations and the initial value)”

R1: 6. *Another example of sloppy writing: Beginning of sect 3.1.3 it reads: “The brine sinking mechanism leads to a larger atmospheric CO_2 increase than iron fertilization (Fig. 2b) with a change of 40 ppm”. This is in detail not correct. The brine sinking mechanism leads to a larger DECREASE in CO_2 than iron fertilisation. Or: The STOPPING of the brine mechanism leads to a larger INCREASE in CO_2 than the STOPPING of the iron fertilisation. Same paragraph: “The response of the system to the abrupt halt of brine sinking takes more time than iron fertilisation. “ Iron fertilisation itself does not take time, CHANGES in the process and its effect of CO_2 might take time.*

Answer: We have changed the sentences as follows:

“**Stopping** the brine sinking mechanism leads to a larger atmospheric CO_2 increase than **stopping**

the iron fertilization”

“The response of the system to the abrupt halt of brine sinking takes more time than **in the case of the iron fertilization.**”

“Hence the time to reach 95% of the equilibrium value is very similar **to the one in the experiment with iron fertilization**”

R1: 7. page 1899, or throughout the results: “upper $\delta^{13}\text{C}_{ocean}$ ” or “deep $\delta^{13}\text{C}_{ocean}$ ” is not a proper wording, it should be “upper ocean $\delta^{13}\text{C}$ ” and “deep ocean $\delta^{13}\text{C}$ ”.

Answer: We have changed “deep/upper $\delta^{13}\text{C}_{ocean}$ ” to “deep/upper ocean $\delta^{13}\text{C}$ ” throughout the text.

R1: 8. page 1900: “When the stratification collapses the diffusion coefficient progressively increases.” This needs explanation.

Answer: We have added a precision:

“When the stratification collapses the diffusion coefficient progressively increases **because the vertical density gradient decreases .**”

R1: 9. sect 3.2: The complete description of the forcing scenarios should be move to sect 2, only results should be seen here.

Answer: Because the forcing scenarios for the brines and iron fertilization change in the different sections, although these two mechanisms were described in the method section, the scenarios for their evolution are explained before giving the results to avoid misunderstanding. The evolution of the other forcings which are always the same are described in the method section.

R1: 10. page 1902, line 1: “the continental shelves are covered simultaneously”. Simultaneously with what?

Answer: With themselves, all at the same time: “If the continental shelves are **all** covered simultaneously”

R1: 11. page 1902, first paragraph. The description including the impact of northern hemispheric ice sheets on sea level needs some refinements.

Answer: This is only a qualitative discussion.

R1: 12. page 1902, lines 22-25: Effect of sea level on nutrients on biological pump versus effect of sea level on salinity: These statements are too general and need some numbers from the analysis of simulation results.

Answer: The effect of changing the background conditions to the climate of the Last Glacial Maximum has already been described in detail in previous studies and is only very briefly reminded to compare the carbon state obtained with the one with other mechanisms. We have added the following sentence: “For more details on these different effects we refer to Brovkin et al. (2007); Bouttes et al. (2010).”

R1: 13. throughout the results: It is not necessary to describe the colour and shape of the figs in the text, it is enough if they are properly label ed in the figs themselves.

Answer: As suggested we have removed the description of the corresponding lines in the figures.

R1: 14. page 1903, lines 20-30: details on the sediment core were already given previously, thus can be omitted here.

Answer: We have removed the details on the location of the sediment core.

R1: 15. Throughout the results and all Tables and Figs: Ocean $\delta_{13}C$: sometimes it is labelled $\Delta\delta_{13}C$ (thus changes in the gradient), sometimes deep ocean $\delta_{13}C$ in the Southern Ocean. It is not clear to the reader if it always refers to the same things (and is incorrectly named sometimes) or if really two different things are meant here. Please carefully crosscheck (e.g. Tab 1 vs Tab 2 to start with).

Answer: We have checked the tables and figure captions.

R1: 16. Fig 14: x axis is reversed with respect to all other figs. Thus, to be consistent I suggest to also let time run from left to right here. Fig 14c is named $\delta^{13}C$, but is in the description only changes in deep ocean $\delta^{13}C$ in the southern Ocean, and not in the gradient, please revise/correct.

Answer: As suggested we have modified the figure to be more consistent with the previous ones. Time goes from the left to the right and we have plotted the ocean $\delta_{13}C$ instead of the vertical gradient.

2 Answer to Reviewer 2

R2: The manuscript describes simulations of the last deglaciation using a coupled climate carbon cycle model. The authors extend their earlier work on the LGM equilibrium change to transient model experiments. Because they have shown earlier that the combination of enhanced salty bottom water formation around Antarctica (the authors suggest it is related to brine release), a stratification dependent vertical diffusivity and iron fertilization can reproduce glacial atmospheric CO_2 and $\delta^{13}C$ in the deep South Atlantic it may not be a big surprise that in transient simulations, in which these three processes change from LGM to early Holocene, the long-term change of observed atmospheric CO_2 and deep South Atlantic $\delta^{13}C$ can be reproduced. Nevertheless, I think the work contributes to the discussion of glacial-interglacial CO_2 change and is well suited for publication in *Climate of the Past*.

I have one major point and several minor ones.

Major point: brine scenario

R2: The major point is related to the brine scenario schematically shown in Fig. 7. I think it is important to realize, and should be made clearer in the manuscript e.g. in the abstract, that this is a hypothetical mechanism. This is not a process that is interactively simulated in the model, but an ad hoc manipulation of deep-water formation in the Southern Ocean. From Fig. 7 I would assume that the deglaciation is a transition from the bottom panel to the top, so that at the glacial maximum (bottom panel) there is no brine water formation, during the deglaciation (middle panel) there is lots of brine water formation and in the Holocene there is little. Thus there should be a peak in brine water formation during the deglaciation, when the shelf is partially flooded. But this sequence of events is inconsistent with the scenario used (Fig. 6), in which bottom water formation is strong during the glacial maximum and decreases during the transition into the Holocene.

Answer: The scenarios that we explore are indeed hypothetic ones and we have made this clearer in the abstract: “In this scenario, we make the hypothesis that sea ice formation was then shifted to the open ocean where the salty water is quickly mixed with fresher water”

As discussed in the manuscript the scenarios that we consider do not take into account a sinking of brines during the deglaciation. Indeed, the deglaciation and glaciation are not symmetrical. During the glaciations the sea level falls gradually whereas it increases more rapidly during the deglaciations. Moreover the Antarctic ice sheet seems to have retreated later than the North Hemisphere ice sheets. Hence the sinking of brines would be inhibited longer. When the Antarctic ice sheet retreats and the sinking becomes possible again the sea level would already be higher and therefore the effect of the sinking of brines would start at a smaller level. In the scenarios studied we do not take this smaller sinking of brines into account for simplicity reasons and because we focus on the general trend, whereas this brief effect of the sinking of brines during the later part of the deglaciation could probably be more related to abrupt events. It is nonetheless an effect that deserves to be studied in more details in the future. To make this clearer we have modified the manuscript as follows:

“Because the glaciation and deglaciation are not symmetrical with respect to the sea level change and advance and retreat of Antarctica on the ice shelves, the evolution of the sinking of brines would also not be symmetrical. In particular, according to data, the Antarctic ice sheet melting starts later than the northern ones, around 14 kyr BP (Clark et al., 2009; Mackintosh et al., 2011). At that time, the already higher sea level (due to the melting of the Northern ice sheets that started earlier) associated to the input of fresh water from the melting of the Antarctic ice sheet can then prevent important sinking of brines to happen again. It is thus not possible to exclude that some sinking of the brines occurred again (although not at the very beginning of the deglaciation since it was inhibited by the presence of the Antarctic ice sheet on the shelves), yet it would be relatively less important. However, this possibility is beyond the scope of this study, which explores the mean trend during the deglaciation, and would require further work to focus on the effect of a brief activation of the sinking of brines during the deglaciation, probably in link with more rapid events.”

Minor points:

R2: 1. Page 1888, line 12: use “coupled climate-carbon”

Answer: It has been changed.

R2: 2. P 1888, l 24: include “long-term” before “CO₂”

Answer: “long-term” has been added.

R2: 3. P 1888, l 25: what data? Specify!

Answer: We have added “ice core” to data.

R2: 4. P 1889, l 28: *The terrestrial biosphere decreases on areas of the continental shelf that become flooded. Cite Montenegro et al. 2006 GRL.*

Answer: As advised we have added the reference to Montenegro et al., 2006: “Furthermore, during the deglaciation the carbon content of the terrestrial biosphere globally increases as the vegetation expands on previously glaciated areas, although it decreases on areas of the continental shelf that become flooded (Montenegro et al., 2006).”

R2: 5. P 1891, l 26: here and elsewhere put a comma in front of “which”

Answer: We have added a comma in front of “which” here and in the rest of the manuscript.

R2: 6. P 1892, subsection 2.2.1: *It should be discussed that this is also a highly idealized ad-hoc treatment of iron fertilization. No iron cycle is used and no realistic dust fluxes.*

Answer: We have added the following sentence to stress the absence of iron cycle in the model, hence the use of the simple parameterization of its effect: “This is a simple parameterization of the effect of iron fertilization as the iron cycle is not simulated in the model.”

R2: 7. P 1893: subsection title: it should be “dependent”

Answer: Here and in the rest of the manuscript we have replaced “dependant” by “dependent”.

R2: 8. I’m missing a description of the $\delta^{13}\text{C}$ model. Please include details such as treatment of biological fractionation in the ocean and on land. Is there a distinction between C3 and C4 plants?

Answer: The description of the model is in Brovkin et al. (2002). We have added this reference in the manuscript. The difference between C3 and C4 for the fractionation is taken into account (the ^{13}C fractionation factor is respectively 0.982 and 0.995 for C3 and C4 plants).

“It includes a carbon cycle model with the fractionation of ^{13}C Brovkin et al. (2002).”

R2: 9. I’m also missing a discussion of the possibility of a larger fixed nitrogen inventory during the LGM. On page 1894 it is mentioned that nutrient concentrations are increased by 3.3%, but NO_3 may have been much more increased because denitrification has been much smaller.

Answer: The nutrient increase has been increased by 3.3% to take into account the change of sea level of around 120m during the LGM compared to the preindustrial. The effect of smaller denitrification is not included.

R2: 10. The discussion of the “Evolution of the forcing” does not mention if Bering Strait is opening during the deglacial or not.

Answer: The geography is not changed between the glacial and preindustrial periods. The effect of the closing and opening of the Bering Strait is thus not taken into account in this study. We have added this precision: “The geography is thus not directly changed and the closing-opening of the Bering Strait is not taken into account.”

R2: 11. P 1900, l 27: insolation does not vary according to proxy data

Answer: We have changed the sentence as follows: “As described in the method section, in these simulations the three boundary conditions that are the atmospheric CO_2 , ice sheets and orbital parameters vary through time. Atmospheric CO_2 and ice sheets vary according to proxy data.”

R2: 12. P 1901, l 8: how exactly is the iron fertilization related to the dust record? Include formula.

Answer: The iron fertilization is just multiplied by a factor between 0 and 1 which follows the iron flux record. We have added more details on this parameterization:

“In the model, it is simply taken into account by forcing the marine biology to use all the nutrients that would otherwise be left in the Atlantic and Indian sectors of the Sub-Antarctic surface ocean (30° S to 50° S) during the glacial period as previously done (Brovkin et al., 2007). **This is a simple parameterization of the effect of iron fertilization as the iron cycle is not simulated in the model. As done in Bouttes et al. (2011), we use a parameter to vary this effect between 0 and 1. This parameter is first set to 1 to explore the maximum potential effect of this mechanism. In the last section we use a combination of the three mechanisms from Bouttes et al. (2011) in which this parameter is set to 0.3.**”

“The evolution of iron fertilization is based on **iron flux** records (Wolff et al., 2006). It is indeed modulated by a parameter *iron* that can evolve between 0 and 1 following the **iron flux record**. **The**

parameter is at its maximum (*iron=1*) at the Last Glacial Maximum and close to 0 at the beginning of the Holocene (Figure 6a).”

R2: 13. P 1901, l 20: *Increased AABW formation due to more sea ice cover at the LGM has been simulated before e.g. in Schmittner (2003, EPSL), which could be cited here.*

Answer: In this section we are discussing the qualitative effect of changing the volume of water above the ice shelf which is a local process and was not studied in Schmittner et al. (2003). Moreover, although the latter brought very interesting results on terms of the effect of the changing sea ice cover on the radiocarbon values it did not explore the effect on CO₂ and does not seem relevant here.

R2: 14. P 1901, l 28-29: *Why is mixing more important in the open ocean. Please include references.*

Answer: As pointed out by the reviewer it is not the mixing which becomes more important, but the dilution of the salty water rejected by sea ice formation. We have thus modified the sentence as follows: “In the open ocean, the dilution of the brines released by sea ice is more important and the effect of the brine-generated dense water disappears.”

R2: 15. P 1902, l 23: *It would be nice if the authors quantified the effect of the 3.3% nutrient increase on glacial CO₂.*

Answer: To evaluate the effect of the 3,3% increase in nutrients we have run an additional control glacial simulation without this increase and find that the atmospheric CO₂ is 3ppm higher. Hence the effect of the 3,3% increase of nutrients in the model is to lower atmospheric by 3ppm which is very small compared to the other processes studied here.

R2: 16. P 1902, l 26: *How was the 650 GtC determined? Was the shelf effect included? (see Montenegro paper mentioned above)*

Answer: The shelf effect was not included as the geography is not changed. We have added the following: “This effect does not take into account the increase of terrestrial biosphere carbon content on shelf areas previously flooded, which would be of around 182-266 GtC (Montenegro et al., 2006).”

R2: 17. P 1903, l 13: *I find it difficult to assess the reliability of the modeled calcium carbonate compensation effect. E.g. could it be sensitive to the details of the circulation that are missing in the ocean model component or is this a rather robust result? Are there modern observations, e.g. percent carbonate in sediments, that the model could or has already been compared to? Perhaps a discussion on this may be helpful.*

Answer: The carbonate compensation model has been discussed and evaluated in Brovkin et al, 2007. We thus refer to this study: “The coupling between CLIMBER-2 and the carbonate compensation model has been discussed in details in Brovkin et al. (2007).”

R2: 18. P 1908, l 4: *“considered”*

Answer: The mistake has been corrected.

R2: 19. P 1909, l 19: *should “K_z” be “alpha”?*

Answer: The parameter which is modified is indeed alpha and not K_z, which has been modified in the manuscript.

R2: 20. P 1910: *There should be a discussion of possible reasons for the maximum in deep ocean*

$\delta^{13}\text{C}$, which is not captured by any of the models.

Answer: Because CLIMBER-2 is an intermediate complexity model with a zonally averaged ocean and low resolution, the comparison of oceanic $\delta^{13}\text{C}$ with the sediment core data is more difficult. Hence we focus primarily on the relative amplitude of the $\delta^{13}\text{C}$ change. A more precise comparison should be obtained with better resolved 3D models, which remains to do with the mechanisms studied here. Although we focus on the general trend of the variables, part of their evolution can also be partly due to more rapid events, which is beyond the scope of this study.

In the manuscript we have added the following: “Although the general trend of the ocean $\delta^{13}\text{C}$ evolution is well simulated with the model, the absolute values are slightly different. Because CLIMBER-2 is an intermediate complexity model with a low resolution and zonally averaged ocean, it complicates the comparison with the sediment core data. Similar experiments exploring the impacts of the sinking of brines with a better resolved 3D ocean model should lead to a better comparison.”

R2: 21. *References: What are the numbers at the end of the references? Figure 5: Caption: The last sentence makes no sense. There is no circulation from south to north.*

Answer: The numbers at the end of the reference should be deleted. The last sentence of the caption has been deleted.

R2: 22. *Figures 8, 10 and 11 should be bigger.*

Answer: In the format of CPD it is not possible to make them larger without erasing the caption but they should be made larger in the final format.

R2: 23. *Fig. 14: include atmospheric C13. Also, a run without carbonate compensation would be informative.*

Answer: We have included atmospheric c13 and the control run without carbonate compensation in Figure 14.

R2: 24. *Adding to point 2 of referee #1: Was radiative forcing of dust included? (see Mahowald et al. 2006 GRL)*

Answer: No, the radiative forcing of dust was not included in this study as discussed in the answer of point 2 from referee 1, but it should be included in future work.

References

- Archer, D., Winguth, A., Lea, D., and Mahowald, N.: What caused the glacial / interglacial pCO_2 cycles?, *Rev. Geophys.*, 38, 159–189, 2000.
- Bopp, L., Kohfeld, K. E., Quéré, C. L., and Aumont, O.: Dust impact on marine biota and atmospheric CO_2 during glacial periods, *Paleoceanography*, 18(2), 1046, doi:10.1029/2002PA000810, 2003.
- Bouttes, N., Roche, D. M., and Paillard, D.: Impact of strong deep ocean stratification on the carbon cycle, *Paleoceanography*, 24, PA3203, doi:10.1029/2008PA001707, 2009.
- Bouttes, N., Paillard, D., and Roche, D. M.: Impact of brine-induced stratification on the glacial carbon cycle, *Clim. Past*, 6, 575–589, doi:10.5194/cpd-6-681-2010, 2010.

- Bouttes, N., Paillard, D., Roche, D. M., Brovkin, V., and Bopp, L.: Last Glacial Maximum CO₂ and $\delta^{13}\text{C}$ successfully reconciled, *Geophys. Res. Lett.*, 38, L02705, doi:10.1029/2010GL044499, 2011.
- Broecker, W. S. and Peng, T.-H.: The Role of CaCO₃ Compensation in the Glacial to Interglacial Atmospheric CO₂ Change, *Global Biogeochem. Cycles*, 1(1), 15–29, 1987.
- Brovkin, V., Bendtsen, J., Claussen, M., Ganopolski, A., Kubatzki, C., Petoukhov, V., and Andreev, A.: Carbon cycle, vegetation, and climate dynamics in the Holocene: Experiments with the CLIMBER-2 model, *Global Biogeochem. Cycles*, 16(4), 1139, doi:10.1029/2001GB001662, 2002.
- Brovkin, V., Ganopolski, A., Archer, D., and Rahmstorf, S.: Lowering of glacial atmospheric CO₂ in response to changes in oceanic circulation and marine biogeochemistry, *Paleoceanography*, 22, PA4202, doi:10.1029/2006PA001380, 2007.
- Brovkin, V., Ganopolski, A., Archer, D., and Munhoven, G.: Glacial CO₂ cycle as a succession of key physical and biogeochemical processes, *Clim. Past Discuss.*, 7, 1767–1795, doi:10.5194/cpd-7-1767-2011, 2011.
- Caillon, N., Severinghaus, J. P., Jouzel, J., Barnola, J.-M., Kang, J., and Lipenkov, V. Y.: Timing of Atmospheric CO₂ and Antarctic Temperature Changes Across Termination III, *Science*, 299, 1728, doi:10.1126/science.1078758, 2003.
- Clark, P. U., Dyke, A. S., Shakun, J. D., Carlson, A. E., Clark, J., Wohlfarth, B., Mitrovica, J. X., Hostetler, S. W., and McCabe, A. M.: The Last Glacial Maximum, *Science*, 325, 710–714, doi:10.1126/science.1172873, 2009.
- Gersonde, R., Crosta, X., Abelmann, A., and Armand, L.: Sea-surface temperature and sea ice distribution of the Southern Ocean at the EPILOG Last Glacial Maximum -a circum-Antarctic view based on siliceous microfossil records, *Quat. Sci. Rev.*, 24, 869–896, 2005.
- Huybrechts, P.: Sea-level changes at the LGM from ice-dynamic reconstructions of the Greenland and Antarctic ice sheets during the glacial cycles, *Quat. Sci. Rev.*, 21 (1-3), 203–231, doi:10.1016/S0277-3791(01)00082-8, 2002.
- Kohfeld, K. E., Quéré, C. L., Harrison, S. P., and Anderson, R. F.: Role of Marine Biology in Glacial-Interglacial CO₂ Cycles, *Science*, 308, 74–78, 2005.
- Köhler, P., Fischer, H., Munhoven, G., and Zeebe, R. E.: Quantitative interpretation of atmospheric carbon records over the last glacial termination, *Global Biogeochem. Cycles*, 19, GB4020, doi:10.1029/2004GB002345, 2005.
- Mackintosh, A., Golledge, N., Domack, E., Dunbar, R., Leventer, A., White, D., Pollard, D., DeConto, R., Fink, D., Zwart, D., Gore, D., and Lavoie, C.: Retreat of the East Antarctic ice sheet during the last glacial termination, *Nature geoscience*, 4, 195–202, doi:10.1038/ngeo1061, 2011.
- Martin, J. H.: Glacial-Interglacial CO₂ change: the iron hypothesis, *Paleoceanography*, 5, 1–13, 1990.
- Montenegro, A., Eby, M., Kaplan, J. O., Meissner, J., and Weaver, A. J.: Carbon storage on exposed continental shelves during the glacial-interglacial transition, *Geophys. Res. Lett.*, 33, L08703, doi:10.1029/2005GL025480, 2006.

- Paillard, D. and Parrenin, F.: The Antarctic ice sheet and the triggering of deglaciations, *Earth Planet. Sci. Lett.*, 227, 263–271, 2004.
- Ritz, C., Rommelaere, V., and Dumas, C.: Modeling the evolution of Antarctic ice sheet over the last 420,000 years: Implications for altitude changes in the Vostok region, *J. Geophys. Res.*, 106, 31,943–31,964, 2001.
- Shemesh, A., Hodell, D., Crosta, X., Kanfoush, S., Charles, C., and Guilderson, T.: Sequence of events during the last deglaciation in Southern Ocean sediments and Antarctic ice cores, *Paleoceanography*, 17 (4), 1056, doi:10.1029/2000PA000599, 2002.
- Skinner, L. C., Fallon, S., Waelbroeck, C., Michel, E., and Barker, S.: Ventilation of the Deep Southern Ocean and Deglacial CO₂ Rise, *Science*, 328 (5982), 1147–1151, doi:10.1126/science.1183627, 2010.
- Tagliabue, A., Bopp, L., Roche, D. M., Bouttes, N., Dutay, J.-C., Alkama, R., Kageyama, M., Michel, E., and Paillard, D.: Quantifying the roles of ocean circulation and biogeochemistry in governing ocean carbon-13 and atmospheric carbon dioxide at the last glacial maximum, *Clim. Past*, 5, 695–706, 2009.
- Toggweiler, J. R.: Variation of atmospheric CO₂ by ventilation of the ocean’s deepest water, *Paleoceanography*, 14(5), 571–588, 1999.
- Tschumi, T., Joos, F., Gehlen, M., and Heinze, C.: Deep ocean ventilation, carbon isotopes, marine sedimentation and the deglacial CO₂ rise, *Clim. Past*, 7, 771–800, doi:10.5194/cp-7-771-2011, 2011.
- von Deimling, T. S., Ganopolski, A., Held, H., and Rahmstorf, S.: How cold was the Last Glacial Maximum?, *Geophys. Res. Lett.*, 33, L14 709, doi:10.1029/2006GL026484, 2006.
- Watson, A. J. and Garabato, A. C. N.: The role of Southern Ocean mixing and upwelling in glacial-interglacial atmospheric CO₂ change, *Tellus B*, 58 (1), 73–87, doi:10.1111/j.1600-0889.2005.00167.x, 2005.
- Wolff, E. W., Fischer, H., Fundel, F., Ruth, U., Twarloh, B., Littot, G. C., Mulvaney, R., Röthlisberger, R., de Angelis, M., Boutron, C. F., Hansson, M., Jonsell, U., Hutterli, M. A., Lambert, F., Kaufmann, P., Stauffer, B., Stocker, T. F., Steffensen, J. P., Bigler, M., Siggaard-Andersen, M. L., Udisti, R., Becagli, S., Castellano, E., Severi, M., Wagenbach, D., Barbante, C., Gabrielli, P., and Gaspari, V.: Southern Ocean sea-ice extent, productivity and iron flux over the past eight glacial cycles, *Nature*, 440, 491–496, doi:10.1038/nature04614, 2006.

Impact of oceanic processes on the carbon cycle during the last termination

N. Bouttes^{1,2}, D. Paillard¹, D. M. Roche^{1,3}, C. Waelbroeck¹, M. Kageyama¹, A. Laurantou⁴, E. Michel¹, and L. Bopp¹

¹Laboratoire des Sciences du Climat et de l'Environnement, IPSL-CEA-CNRS-UVSQ, UMR 8212, Centre d'Etudes de Saclay, Orme des Merisiers bat. 701, 91191 Gif Sur Yvette, France.

²NCAS-Climate, Meteorology Department, University of Reading, Reading RG66BB, United Kingdom.

³Faculty of Earth and Life Sciences, Section Climate Change and Landscape dynamics, Vrije Universiteit Amsterdam, De Boelelaan, 1085, 1081 HV Amsterdam, The Netherlands.

⁴LOCEAN, University Paris VI, Paris, France

Correspondence to: N. Bouttes
(n.bouttes@reading.ac.uk)

1

Abstract

During the last termination (from $\sim 18,000$ years ago to $\sim 9,000$ years ago) the climate significantly warmed and the ice sheets melted. Simultaneously, atmospheric CO_2 increased from ~ 190 ppm to ~ 260 ppm. Although this CO_2 rise plays an important role in the deglacial warming, the reasons for its evolution are difficult to explain. Only box models have been used to run transient simulations of this carbon cycle transition, but by forcing the model with data constrained scenarios of the evolution of temperature, sea level, sea ice, NADW formation, Southern Ocean vertical mixing and biological carbon pump. More complex models (including GCMs) have investigated some of these mechanisms but they have only been used to try and explain LGM versus present day steady-state climates.

In this study we use a **coupled climate-carbon** model of intermediate complexity to explore the role of three oceanic processes in transient simulations: the sinking of brines, stratification-dependent diffusion and iron fertilization. Carbonate compensation is accounted for in these simulations. We show that neither iron fertilization nor the sinking of brines alone can account for the evolution of CO_2 , and that only the combination of the sinking of brines and interactive diffusion can simultaneously simulate the increase in deep Southern Ocean $\delta^{13}\text{C}$. The scenario that agrees best with the data takes into account all mechanisms and favours a rapid cessation of the sinking of brines around 18,000 years ago, when the Antarctic ice sheet extent was at its maximum. In this scenario, we make the hypothesis that sea ice formation was then shifted to the open ocean where the salty water is quickly mixed with fresher water, which prevents deep sinking of salty water and therefore breaks down the deep stratification and releases carbon from the abyss. Based on this scenario it is possible to simulate both the amplitude and timing of the **long-term** CO_2 increase during the last termination in agreement with **ice core** data. The atmospheric $\delta^{13}\text{C}$ appears to be highly sensitive to changes in the terrestrial biosphere, underlining the need to better constrain the

2

vegetation evolution during the termination.

1 Introduction

The last termination, which took place between $\sim 18,000$ and $\sim 9,000$ years ago, is characterized by a global warming (Visser et al., 2003; North Greenland Ice Core Project members, 2004; EPICA community members, 2004; Barker et al., 2009) associated to a shrinking of the ice sheets (Peltier, 1994, 2004; Svendsen et al., 2004). The climate evolved from a cold glacial state (sea surface temperature of -2 to -6°C cooler relative to today in the Southern Ocean (MARGO Project Members, 2009)) associated with large northern hemisphere ice sheets covering large parts of Europe and North America (Peltier, 2004), to a warmer interglacial state with reduced ice sheets, similar to the modern ones.

The warming in Antarctica is tightly linked to an atmospheric CO_2 increase from ~ 190 ppm at the Last Glacial Maximum (LGM, $\sim 21,000$ years ago) to ~ 260 ppm at the beginning of the Holocene ($\sim 9,000$ years ago) (Monnin et al., 2001; Laurantou et al., 2010). The CO_2 rise is crucial to explain the warming and shrinking of ice sheets (Berger et al., 1998; Charbit et al., 2005; Ganopolski et al., 2010), in association with the change of insolation. Yet explaining such an increase remains a challenge.

Moreover, the isotopic composition of carbon ($\delta^{13}\text{C}$) both in the atmosphere and ocean also evolves during the transition, providing clues and constraints on the evolution of the carbon cycle. The atmospheric $\delta^{13}\text{C}$ ($\delta^{13}\text{C}_{atm}$) presents a W-shape with two negative excursions of 0.5‰ during Heinrich event 1 (H1) and the Younger Dryas (YD) (Laurantou et al., 2010). In the ocean the vertical gradient of $\delta^{13}\text{C}_{ocean}$ (the gradient between the upper (-2000 m to 0 m) and the deep (-5000 m to -3000 m) ocean $\Delta\delta^{13}\text{C}_{ocean} = \delta^{13}\text{C}_{upper} - \delta^{13}\text{C}_{bottom}$) decreases both in the South and North Atlantic. In particular the deep South Atlantic values increase from around -0.8 permil at the LGM

3

to around 0.4 permil in the modern ocean (Hodell et al., 2003; Curry and Oppo, 2005), and more locally from around -1 permil to around 0 permil at location of core MD07-3076Q (44°S , 14°W , -3770m) (Skinner et al., 2010; Waelbroeck et al., in press).

Furthermore, during the deglaciation the carbon content of the terrestrial biosphere globally increases as the vegetation expands on previously glaciated areas, although it decreases on areas of the continental shelf that become flooded (Montenegro et al., 2006). The general warming generates a migration of ecosystems towards the poles while the rise of CO_2 favours the uptake of carbon by plants (Kaplan et al., 2002; Köhler and Fischer, 2004). Carbon storage by the terrestrial biosphere from the LGM to the Pre-industrial is estimated by vegetation models to be between 600 GtC and 821 GtC (Kaplan et al., 2002; Brovkin et al., 2002b; Köhler and Fischer, 2004). Reconstructions based on proxy data estimate the range of possible terrestrial carbon change to be 270-720 GtC from marine records (Bird et al., 1994), and 750 -1050 GtC from pollen based estimations (Crowley, 1995).

Since both the atmosphere and the terrestrial biosphere carbon contents increase during the termination, it is generally concluded that the ocean, the largest of the three reservoirs, must be the one that loses carbon. Various hypotheses have been proposed to explain the atmospheric CO_2 increase based on modifications of the oceanic carbon content. Most of them focus either on changes in the dynamics of the ocean or on modifications of the marine biology (Archer et al., 2000; Sigman and Boyle, 2000; Fischer et al., 2010; Sigman et al., 2010). Yet the tight link between Antarctic temperature and CO_2 (Cuffey and Vimeux, 2001) suggests a simple mechanism instead of a complex association of numerous independent processes. Besides, many of them have been discarded or only account for a small CO_2 change such as the coral reef hypothesis (Berger, 1982; Broecker and Peng, 1982; Opdyke and Walker, 1992; Köhler et al., 2005a), modification of winds (Toggweiler et al., 2006; Menviel et al., 2008a), or sea ice extension (Stephens and Keeling, 2000; Archer et al., 2003), as they required

4

unrealistic changes to account for most of the glacial-interglacial CO₂ change. Other mechanisms have been confirmed. Enhanced marine biology by iron fertilization **during glacial period, which would then decrease during the deglaciation**, is assumed to play a role (Martin, 1990), although of relatively small importance as it could account for a 15-20 ppm **change** (i.e. approximately 20 % of the ~90 ppm total **CO₂ change**) (Bopp et al., 2003; Tagliabue et al., 2009). Carbonate compensation is a recognized process that amplifies the uptake **or loss** of carbon by the ocean (Broecker and Peng, 1987; Archer et al., 2000; Brovkin et al., 2007). Finally, changes in the oceanic circulation and mixing can have a significant impact on glacial CO₂ (Toggweiler, 1999; Paillard and Parrenin, 2004; Köhler et al., 2005a; Watson and Garabato, 2005; Bouttes et al., 2009; Skinner et al., 2010). In particular, it has been recently shown that the deep stratification induced by enhanced brine sinking can strongly decrease CO₂ during the LGM **relative to the Pre-industrial** and simultaneously increase the upper to deep **ocean $\delta^{13}\text{C}$** gradient, in line with data (Bouttes et al., 2010, 2011).

Moreover, if the sinking of brines is not taken into account, the already tested mechanisms are not sufficient to explain the entire glacial **-interglacial CO₂ change** in models of intermediate complexity (EMICs) or General Circulation Models (GCMs), as there is no physical mechanism to account for a sufficient **glacial** deep stratification and reduced circulation. Only box models have been able to perform a simulation of the last termination carbon cycle evolution, by imposing the evolution of the oceanic circulation and mixing inferred from proxy data (Köhler et al., 2005a). Yet box models can be over-sensitive to changes in high latitudes (Archer et al., 2003). Additionally, because of their simplicity the reasons for such changes in mixing and circulation that are crucial for the amplitude of the CO₂ change (more than 45 ppm of the ~90 ppm change (Köhler et al., 2005a)) could not be tested.

In this study we use a climate model of intermediate complexity to explore the impact of two main oceanic mechanisms during the termination: the sinking of brines,

5

which alters the circulation and mixing of water masses and has not yet been tested in transient simulations, and iron fertilization. Two other processes that are not independent are also considered: the amplification of the effects of the sinking of brines by its feedback on diffusion and the amplification of the oceanic uptake of carbon by the carbonate compensation mechanism.

2 Methods

2.1 The Earth system Model of Intermediate Complexity CLIMBER-2

We use the CLIMBER-2 coupled intermediate complexity model (Petoukhov et al., 2000; Ganopolski et al., 2001), which is well suited to perform the long runs of several thousands of years requested to study the deglaciation. CLIMBER-2's atmosphere has a coarse resolution of 10° in latitude by 51° in longitude, which is precise enough to take into account geographical changes, while allowing the model to be fast enough to run long simulations. The ocean is subdivided into three zonally averaged basins with a resolution of 21 depth levels by 2.5° latitude. **It includes a carbon cycle model with the fractionation of ^{13}C (Brovkin et al., 2002a)**. In addition to modules simulating the ocean, atmosphere and continental biosphere dynamics, the model also includes a model of carbonate compensation (Brovkin et al., 2007; Archer, 1991). **The coupling between CLIMBER-2 and the carbonate compensation model has been discussed in details in Brovkin et al. (2007)**. Moreover, three mechanisms are added in the present study: the sinking of brines, iron fertilization and stratification-dependent diffusion.

6

2.2 Additional mechanisms

2.2.1 Iron fertilization

Iron fertilization relies on the removal of the iron limitation in the “High Nutrient Low Chlorophyll” (HNLC) areas thanks to the supply of glacial atmospheric dust which contains iron (Martin, 1990; Bopp et al., 2003; Brovkin et al., 2007; Tagliabue et al., 2009). According to proxy-based study of the change of productivity this effect would have been restrained to the areas north of the modern-day Antarctic polar front (Kohfeld et al., 2005). In the model, it is simply taken into account by forcing the marine biology to use all the nutrients that would otherwise be left in the Atlantic and Indian sectors of the Sub-Antarctic surface ocean (30° S to 50° S) during the glacial period as previously done (Brovkin et al., 2007). This is a simple parameterization of the effect of iron fertilization as the iron cycle is not simulated in the model. As done in Bouttes et al. (2011), we use a parameter to vary this effect between 0 and 1. This parameter is first set to 1 to explore the maximum potential effect of this mechanism. In the last section we use a combination of the three mechanisms from Bouttes et al. (2011) in which this parameter is set to 0.3.

2.2.2 Sinking of brines

The version of CLIMBER-2 used here contains a parameterization of the sinking of brines that has been studied in LGM conditions (Bouttes et al., 2010). Brines are small pockets of very salty water rejected by sea ice formation as sea ice is mainly formed of fresh water. In the standard version of CLIMBER-2 the flux of salt rejected to the ocean is mixed in the surface oceanic cell whose volume is quite large due to the coarse resolution. Yet as brines are very dense because of their high salt content, instead of this dilution they should rapidly sink to the deep ocean where the local topography permits it. During glacial periods the Antarctic ice sheet progressively extends and covers the

7

continental shelves. In combination with the concomitant sea level fall due to increasing ice sheets volume, it leads to a reduction of the volume of water above the continental shelf. The brines rejected from the intense sea ice formation are less diluted and are released closer to the shelf break. The dense water from brines can then more easily sink along the continental slope to the deep ocean. To avoid the dilution of such an effect the sinking of brines to the deep ocean has been parameterized in CLIMBER-2 (Bouttes et al., 2010). The relative importance of this brine mechanism is set by the parameter $frac$, which is the fraction of salt rejected by sea ice formation that sinks to the bottom of the ocean. The rest of the salt ($1 - frac$) is diluted in the corresponding surface oceanic cell as done in the standard version. When $frac = 0$ no salt sinks to the abyss as it is entirely mixed in the surface oceanic cell (control simulation), whereas $frac = 1$ is the maximum effect of the brine mechanism when all the rejected salt sinks to the bottom of the ocean. This mechanism was shown to result in a net glacial atmospheric CO₂ decrease relative to the Pre-industrial as well as increased $\Delta\delta^{13}C_{ocean}$ and increased atmospheric $\delta^{13}C_{atm}$ (Bouttes et al., 2010, 2011).

2.2.3 Stratification-dependent diffusion

As the sinking of brines tends to modify the stratification state of the ocean (the deep water becomes denser) it should modify the vertical diffusion. The more stratified the ocean becomes, the more energy it requires to mix water masses, implying a lower diffusion. Yet in the standard version of CLIMBER-2 the vertical diffusion coefficient K_z is set by a fixed profile and cannot evolve. A parameterization of the vertical diffusion coefficient was therefore introduced (Bouttes et al., 2010) so that vertical diffusion becomes interactive and dependent of the stratification state of the ocean. This allows a more physical representation of the diffusion, which can play a significant role for the ocean circulation (Marzeion et al., 2007) and potentially influence the carbon cycle (Bouttes et al., 2009). The physical parameterization of the vertical diffusion coefficient K_z was introduced depending on the vertical density gradient (Marzeion et al., 2007) in

8

the deep ocean (below 2000m) as follow:

$$K_z \propto N^{-\alpha} \quad (1)$$

where α is a parameter and $N = \left(-\frac{g}{\rho_0} \frac{\partial \rho}{\partial z}\right)^{\frac{1}{2}}$ is the local buoyancy frequency, with g the gravity acceleration, ρ_0 a reference density, and $\frac{\partial \rho}{\partial z}$ the vertical density gradient. The parameter α controls the sensitivity of the vertical diffusivity to changes in stratification. A previous study exploring its role during the LGM has shown that it could vary between 0.7 and 0.9 (Bouttes et al., 2011). We first use the maximum value of 0.9 to test the maximum impact of this mechanism. In the last section we use a combination of the three mechanisms from Bouttes et al. (2011) where $\alpha=0.7$.

The impact of the evolution of these mechanisms is first studied in an idealized case with a fixed climate (set to the LGM) to assess the effect of each of the mechanisms without the complication of a changing climate. We then explore the evolution of the carbon cycle when the climate evolves from the LGM to the Holocene. To disentangle the effects of the ocean and vegetation, the simulations are run with either interactive or fixed vegetation ("fixed veg").

2.3 Initial conditions

The transient simulations start from initial values taken from equilibrium simulations of the Last Glacial Maximum climate and carbon cycle state (Bouttes et al., 2011). The LGM conditions simultaneously imposed in all equilibrium simulations are the 21 kyr BP insolation (Berger, 1978), LGM ice sheets (Peltier, 2004), and atmospheric CO₂ for the radiative code (190 ppm (Monnin et al., 2001; Lourantou et al., 2010)). The atmospheric CO₂ concentration is prescribed in the radiative code in order to correctly simulate the climate as previously done (Brovkin et al., 2007). The model is thus semi-coupled with respect to the climate and carbon cycle. To account for a glacial sea level fall of ~120 m, salinity and mean nutrient concentrations are increased by 3.3%

9

(Brovkin et al., 2007). To ensure equilibrium for the carbon cycle, glacial simulations were run for 50,000 years. The transient simulations analysed in this study start from the equilibrium state of these 50,000 year LGM simulations.

At the end of the 50,000 year simulation, the global mean air temperature with the preindustrial boundary conditions is 12.9°C. With the LGM conditions, the climate is 3.3°C colder. The effect of the dust is not taken into account in this study. According to von Deimling et al. (2006), it would cool the global climate by an additional 1.35±0.35°C, yielding an approximately 4.65±0.35°C colder climate during the LGM compared to the preindustrial. It is in the lower range of the estimation from von Deimling et al. (2006), but the corresponding sea surface temperature change, which is -2°C for the LGM, is in good agreement with the MARGO database (-1.9°C).

With no additional mechanism nor carbonate compensation the obtained LGM CO₂ is around 300 ppm. When carbonate compensation is taken into account, CO₂ is approximately 260 ppm. In the other simulations carbonate compensation is always included. With iron fertilization the LGM CO₂ is around 230 ppm, it falls to around 215 ppm with the sinking of brines. For the stratification-dependent diffusion, the α parameter is first set to its maximum value inferred from a previous study, i.e. 0.9 (Bouttes et al., 2011). The 190 ppm level is reached with either the sinking of brines combined with the stratification-dependent diffusion or the sinking of brines with iron fertilization.

2.4 Evolution of the forcing

During deglaciation, the insolation, sea level, ice sheets and CO₂ evolved. The insolation evolution is calculated from Berger (1978). In the first part of this study, the CO₂ evolution (Monnin et al., 2001; Lourantou et al., 2010) is imposed for the climate modules of the model as it is used to compute the changing radiative forcing, but is not used for the carbon cycle part of the model. CH₄ and N₂O are not explicitly considered in the

model, but the CO₂ is an “equivalent CO₂” that considers the change of CH₄ and N₂O (Brovkin et al., 2007) . Prescribing the CO₂ level allows to obtain a coherent climate even when the CO₂ calculated by the carbon cycle is different from the one recorded in ice cores. In the second part, the model is used in an interactive mode, i.e. the CO₂ calculated by the carbon cycle module is now used to compute the radiative scheme, no CO₂ value is prescribed.

The sea level change is taken into account by changing the global mean salinity and nutrient concentrations based on sea level data (Waelbroeck et al., 2002). This is a global effect that does not take into account addition of fresh water fluxes in restricted areas. Indeed, although abrupt events took place during the last termination (Keigwin et al., 1991), rapid climate changes that can be triggered by the addition of fresh water fluxes (Ganopolski and Rahmstorf, 2001) are beyond the scope of this study, which focuses on the general trends during the transition. **The geography is thus not directly changed and the closing-opening of the Bering Strait is not taken into account.**

The ice sheet evolution is simply imposed by interpolation between LGM and Late Holocene states based on the sea level data. First, a sea level coefficient is computed:

$$sl_{coeff} = \frac{sl - sl_{ctrl}}{sl_{lgm} - sl_{ctrl}} \text{ and } 0 < sl_{coeff} < 1 \quad (2)$$

with sl the sea level of the considered time step, sl_{ctrl} the modern sea level and sl_{lgm} the LGM sea level. Then, from sl_{coeff} we compute the area of the northern hemisphere ice sheets in a given latitudinal sector as:

$$area_{lgm} \times sl_{coeff}^{\frac{2}{3}} \quad (3)$$

with $area_{lgm}$ the LGM ice sheets area (Peltier, 2004). The northern limit of the ice sheets is given by the CLIMBER-2 continental limit. The southern limit is computed

11

from this area. The height of the ice sheets is calculated as:

$$oro_{ctrl} + (oro_{lgm} - oro_{ctrl}) \times sl_{coeff}^{\frac{1}{3}} \quad (4)$$

with oro_{ctrl} the modern orography and oro_{lgm} the LGM orography (Peltier, 2004). This very simple ice sheet evolution formulation was initially developed for longer term simulations for which no information about ice sheet extent and height was precisely known. It provides an ice sheets evolution consistent with the sea level evolution. Such a parameterization should allow the study of a full glacial-interglacial cycle in the future.

In the following we test three oceanic mechanisms (iron fertilization, sinking of brines and stratification-dependent diffusion). We explore different scenarios for their evolution in order to simulate the CO₂ and atmospheric and oceanic $\delta^{13}\text{C}$ evolution during the last deglaciation, and compare the results with proxy data to constrain the possible scenarios.

3 Results and discussion

3.1 Evolution of the mechanisms under a constant LGM climate: sensitivity studies

We first analyze sensitivity studies to compare the impact of the mechanisms (with different scenarios) on the evolution of the carbon cycle with a constant climate and assess the role of each mechanism alone. In these idealized simulations the climate is set by glacial boundary conditions. Atmospheric CO₂ is prescribed to 190 ppm (Monnin et al., 2001); the northern ice sheets (Peltier, 2004) and the orbital parameter values (Berger, 1978) correspond to the situation at 21 kyr BP.

12

3.1.1 Scenarios for the sinking of brines and iron fertilization

Two idealized scenarios are tested for the evolution of the sinking of brines and iron fertilization (Figure 1). Both mechanisms are active at the beginning of the simulations, and then stopped. This halt can either be instantaneous (scenario “abrupt”) or linear in time (scenario “linear”). The evolution imposed for the brines and iron mechanism is the same so that we can compare their responses in time.

3.1.2 Impact of stopping iron fertilization

The halt of iron fertilization leads to an increase of atmospheric CO₂ as the biological pump is weakened (Figure 2 a). CO₂ increases by 29 ppm (Table 1) in both scenarios. The equilibrium is rapidly reached for the abrupt halt of iron fertilization (Scenario “abrupt”). **To compare the time needed by the system to reach a near-equilibrium state we consider the time when the anomaly of a considered variable (defined as the difference between its value and its initial value) has reached 95% of the anomaly of the equilibrium state (Table 2).** In the “abrupt” scenario the system has reached 95% of the equilibrium value ~100 years after the stop of fertilization, i.e. very quickly compared to the time scale of the termination (a few thousand years). In the “linear” scenario, the response of the carbon cycle follows the forcing and it takes ~4400 years for the system to reach 95% of the equilibrium value.

The impact of iron fertilization on $\delta^{13}\text{C}_{\text{ocean}}$ is very small (Figure 3 a). We consider the mean vertical gradient ($\Delta\delta^{13}\text{C}_{\text{ocean}}$) of $\delta^{13}\text{C}_{\text{ocean}}$ in the Atlantic between the upper (-2000m to 0m) and deep (-5000m to -3000m) ocean. The modification of the gradient is only ~0.1 permil (Table 1). On the other hand, the change of $\delta^{13}\text{C}_{\text{atm}}$ is larger (Figure 4 a) as it is decreased by 0.25 permil (Table 1).

13

3.1.3 Impact of stopping the sinking of brines

Stopping the brine sinking mechanism leads to a larger atmospheric CO₂ increase than **stopping the iron fertilization** (Figure 2 b) with a change of 40 ppm (Table 1). **This effect of the brine sinking is not the maximum possible effect (which would be obtained for $frac=1$), but corresponds to a more realistic case ($frac=1$ is very idealistic as it would require no mixing at all) with $frac=0.6$, which is in the middle of the range of probable values according to proxy data (Bouttes et al., 2011).** The response of the system to the abrupt halt of brine sinking takes more time than in the case of the iron fertilization. In the abrupt scenario, 95% of the equilibrium value is reached 900 years after the stop (Table 2). Indeed, the brine sinking mechanism involves changes in the thermohaline circulation through enhanced vertical stratification (Bouttes et al., 2010). The thermohaline circulation takes more time to equilibrate than the biological activity. Halting the sinking of brines stops the transport of salt to the deep ocean. This transport of salt during the glacial period is responsible for a density increase of the deep waters compared to upper waters and therefore a greater vertical stratification **relative to the Pre-industrial**. This leads to a more isolated **glacial** deep water mass that can store a larger amount carbon. When the vertical salt transport is stopped, the stratification breaks down and the thermohaline circulation changes: both the North Atlantic and Southern ocean overturning cells become more vigorous (Figure 5). **Indeed, with the stratification induced by the sinking of brines the maximum of the NADW export is around 15 Sv compared to around 20 Sv without it. When the stratification breaks down the formation of deep water intensifies rapidly to 22 Sv in around 1500 years. It then decreases more slowly back to 20 Sv.** The atmospheric CO₂ follows the evolution of the oceanic circulation as the carbon stored in the abyss is progressively released when the overturning circulation increases.

In the “linear” scenario the thermohaline circulation has more time to adapt and the evolution is smoother. **The maximum export of NADW increases gradually from 15 Sv**

14

to around 20 Sv, the latter being reached after around 4500 years (Figure 5). Hence the time to reach 95% of the equilibrium value is very similar to the one in the experiment with iron fertilization (~4400 years, Table 2).

The amplitude of the $\Delta\delta^{13}\text{C}_{ocean}$ decrease is more significant with the brine sinking mechanism than with the iron fertilization mechanism (Figure 3), with a decrease of the vertical gradient of ~ 0.57 permil. The induced stratification has a large impact on the vertical $\delta^{13}\text{C}_{ocean}$ gradient as it reduces the mixing between the ^{13}C enriched upper water and ^{13}C depleted deep waters. As a result, it better preserves the vertical gradient due to biological activity (Bouttes et al., 2010). In contrast, the change in $\delta^{13}\text{C}_{atm}$ is similar to the one induced by suppression of the iron fertilization. The sinking of brines has an important impact on both $\Delta\delta^{13}\text{C}_{ocean}$ and $\delta^{13}\text{C}_{atm}$ because it efficiently increases upper ocean $\delta^{13}\text{C}$ and decreases deep ocean $\delta^{13}\text{C}$. When the stratification breaks down it thus leads to a decrease of upper ocean $\delta^{13}\text{C}$ and $\delta^{13}\text{C}_{atm}$. The iron fertilization mechanism has a smaller effect on $\Delta\delta^{13}\text{C}_{ocean}$ partly because remineralization not only takes place in the deep ocean, but also above. Even if the surface $\delta^{13}\text{C}_{ocean}$ is significantly increased with iron fertilization (as well as $\delta^{13}\text{C}_{atm}$), the deep (-5000 m to -3000 m) $\delta^{13}\text{C}_{ocean}$ is relatively less modified (the remineralization also releases ^{12}C in intermediate waters) and therefore $\Delta\delta^{13}\text{C}_{ocean}$ changes less than with the sinking of brines.

3.1.4 Impact of stopping the sinking of brines with the stratification-dependent diffusion included

The addition of the stratification-dependent diffusion mainly amplifies the impact of the brine sinking mechanism. Because of the lower vertical diffusion induced by the enhanced vertical density gradient, the deep water mass is even more isolated at the beginning of the simulation. It yields a lower initial CO_2 level (Figure 2 c), higher initial $\Delta\delta^{13}\text{C}_{ocean}$ (Figure 3 c) (Bouttes et al., 2011) and higher initial $\delta^{13}\text{C}_{atm}$ (Figure 4 c).

15

When the brine sinking stops it thus leads to a larger CO_2 increase reaching 61 ppm (Table 1).

Moreover, the interactive diffusion induces a delay in the oceanic circulation response. After a first rapid increase of the export of North Atlantic Deep Water similar to the one in the simulation without the interactive diffusion (it reaches 20 Sv after around 500 years), the maximum export of NADW very slowly increases of around 1 Sv in around 3500 years (Figure 5). As the stratification breaks down the diffusion coefficient, which is interactively computed, increases as well. Because the mixing increases it tends to diminish the density gradient and the export of water. As a consequence it leads to the same delay in the carbon evolution. Indeed, with the interactive diffusion the diffusion coefficient is lower at the beginning of the simulation because of the enhanced stratification. When the stratification collapses the diffusion coefficient progressively increases because the vertical density gradient decreases. Yet it remains smaller than in the simulation without interactive diffusion (until the vertical density gradient is the same), so that the mixing is less important and the change of circulation smaller than in the fixed diffusion simulation. Because of this delay, the CO_2 reaches 95% of the equilibrium value $\sim 4,300$ years after the sudden halt of brine sinking, i.e. $\sim 3,400$ years later than with the brines mechanism alone. Similarly, in the “linear” scenario it takes $\sim 7,400$ years for the system to reach 95% of the equilibrium value, i.e. $\sim 3,100$ years later compared to the brines alone.

The halt of the sinking of brines with the stratification-dependent diffusion also leads to a decrease of both $\delta^{13}\text{C}_{atm}$ and $\Delta\delta^{13}\text{C}_{ocean}$. The amplitude is slightly greater than with brines alone for $\delta^{13}\text{C}_{atm}$ (change of 0.34 permil, Table 1) because of the amplification due to the interactive diffusion. The amplitude is however much higher for $\Delta\delta^{13}\text{C}_{ocean}$ with the interactive diffusion, which plays an important role in the ocean. It isolates even more the deep ocean, which strongly decreases the deep ocean $\delta^{13}\text{C}$. The additional delay because of the progressive return to modern diffusion values is

apparent in both cases with $\delta^{13}\text{C}$ reaching 95% of the equilibrium value approximately 3,800-3,900 years later than with brines alone. In the “linear” scenario the ocean has more time to adapt and this delay is reduced to 2,500-2,700 years.

3.2 Evolution of the mechanisms during the last deglaciation with prescribed CO_2

We now consider iron fertilization and the sinking of brines in the context of the global warming and ice sheet retreat of the last deglaciation. As described in the method section, in these simulations the three boundary conditions that are the atmospheric CO_2 , ice sheets and orbital parameters vary through time. Atmospheric CO_2 and ice sheets vary according to proxy data. The vegetation is either interactively calculated by the terrestrial biosphere model (VECODE) and therefore evolving with time according to the climate and CO_2 concentration imposed, or fixed to the glacial distribution as calculated in the glacial simulations (“fixed veg”) in order to separate the impact of the ocean from the one of the vegetation. Iron fertilization and the sinking of brines follow different scenarios (Figure 6). The evolution of iron fertilization is based on iron flux records (Wolff et al., 2006). It is indeed modulated by a parameter *iron* that can evolve between 0 and 1 following the iron flux record. The parameter is at its maximum (*iron*=1) at the Last Glacial Maximum and close to 0 at the beginning of the Holocene (Figure 6a). The evolution of the sinking of brines (which can not be directly constrained) is set by the same two idealised scenarios as in the previous part.

The halt of the sinking of brines imposed in the model would in reality be due to the change of topography around Antarctica (Figure 7). Indeed, the sinking of brines would depend on the volume of water above the shelves. It would thus depend on two variables: the evolution of sea level and the advance/retreat of the Antarctic ice sheet on the shelves. During interglacials, the volume of water above the continental shelves is important and some mixing of the salt rejected by sea ice formation happens. The

17

salty dense water can thus not easily sink to the bottom of the ocean (Figure 7a). During the glaciation, the Antarctic ice sheet progressively increases both in volume and extension (Figure 7b). Because of the extension of the ice sheet and the sea level fall, the volume of water above the Antarctic ice shelves is reduced and the salt less diluted. Moreover, the release of salt increases as more sea ice is formed (in particular as the seasonality seems to increase (Gersonde et al., 2005)). The salt rejected by sea ice formation can accumulate more and create very dense water susceptible to flow more easily down to the abyss. This is modelled by an increase of the fraction of salt that sinks to the deep ocean, the *frac* parameter. When the ice sheet reaches its maximum extent, i.e. when the continental shelves are covered, a few thousand years after the Last Glacial Maximum (Ritz et al., 2001; Huybrechts, 2002), the sea ice formation is shifted to the open ocean. The absence of shelf where the brines sink, accumulate and create very dense water susceptible to flow down to the abyss, prevents the deep sinking of brines (Figure 7c). In the open ocean, the dilution of the brines released by sea ice is more important and the effect of the brine-generated dense water disappears. If the continental shelves are all covered simultaneously it results in an abrupt halt of the sinking of brines. Alternatively, the halt of the sinking of brines can be linked to the sea level rise, which increases the volume of water above the continental shelf leading to more mixing and less sinking of dense water. It corresponds to a more progressive reduction of the sinking of brines, which can be first approximated by a linear decrease. These two extreme scenarios (“linear” and “abrupt”) of the halt of the sinking of brines are both tested. The two scenarios explore the two extreme cases, a more probable one would lie between the two. Because the glaciation and deglaciation are not symmetrical with respect to the sea level change and advance and retreat of Antarctica on the ice shelves, the evolution of the sinking of brines would also not be symmetrical. In particular, according to data, the Antarctic ice sheet melting starts later than the northern ones, around 14 kyr BP (Clark et al., 2009; Mackintosh et al., 2011). At that time, the already higher sea level (due to the melting of the Northern ice sheets that started earlier) associated to the input of fresh water from the melting of the Antarctic ice sheet

can then prevent important sinking of brines to happen again. It is thus not possible to exclude that some sinking of the brines occurred again (although not at the very beginning of the deglaciation since it was inhibited by the presence of the Antarctic ice sheet on the shelves), yet it would be relatively less important. However, this possibility is beyond the scope of this study, which explores the mean trend during the deglaciation, and would require further work to focus on the effect of a brief activation of the sinking of brines during the deglaciation, probably in link with more rapid events.

3.2.1 Control simulations of the evolution of the carbon cycle during the deglaciation

Without carbonate compensation, the initial value of atmospheric CO₂ at -21,000 years is 300 ppm (Figure 8 a) due to the opposite effects of oceanic and vegetation changes (Brovkin et al., 2007; Bouttes et al., 2010). Because of the colder climate, the solubility of CO₂ is greater in the glacial ocean compared to the Holocene, which results in low atmospheric CO₂. The increase of nutrient concentrations due to the sea level fall of approximately 120 m also reduces CO₂ relative to the Pre-industrial since the biological production is enhanced. Yet the sea level fall also increases the global oceanic salinity, which decreases CO₂ solubility in the ocean thus increases CO₂. Finally, the terrestrial biosphere carbon content is reduced by ~650 GtC compared to the Holocene (Figure 9), which releases carbon into the atmosphere. This effect does not take into account the increase of terrestrial biosphere carbon content on shelf areas previously flooded, which would be of around 182-266 GtC (Montenegro et al., 2006). Although the ocean partially stores some of the released carbon, part of it remains in the atmosphere. This effect prevails and the simulated atmospheric CO₂ is 300 ppm at the LGM, a value very different from the data (~190 ppm). For more details on these different effects we refer to Brovkin et al. (2007); Bouttes et al. (2010).

From this initial state, in the control glacial simulation without carbonate compensa-

19

tion (CTRL) the atmospheric CO₂ slightly decreases from 300 ppm 21,000 years ago to 280 ppm 10,000 years ago when the terrestrial biosphere evolution is taken into account (Figure 8 a) whereas CO₂ increases to 320 ppm when the vegetation is fixed. CO₂ increases because of the warming and diminished global oceanic nutrient concentrations. The decrease of salinity tends to counteract the increase, but the overall evolution is still a CO₂ increase when the vegetation is fixed (“fixed veg”). When the evolution of vegetation is accounted for (interactive vegetation) it results in a CO₂ decrease as the terrestrial biosphere carbon content progressively increases (Figure 9). This effect prevails leading to the simulated decrease of atmospheric CO₂.

With carbonate compensation (CTRL-CC) the uptake of carbon by the ocean is amplified during the LGM, which results in a lower glacial CO₂ in the initial state, around 260 ppm (Figure 8a). When the vegetation is fixed, the evolution of CO₂ in the transient simulation is the same as in the previous simulation with a 20 ppm increase. When the vegetation is interactive, the CO₂ remains roughly constant because the terrestrial biosphere carbon content increases, which acts to decrease CO₂ and counteracts the CO₂ increase from oceanic processes.

The evolution of $\delta^{13}\text{C}_{ocean}$ in the ocean is a good indicator of the physical processes involved and an important constraint. One of the more striking features of the changes from the glacial to the interglacial state is the increase in the deep Southern Ocean $\delta^{13}\text{C}_{ocean}$ value, hence we focus on the evolution of $\delta^{13}\text{C}$ at one site in the deep Southern Ocean. We compare the simulation results to the record from core MD07-3076Q (Skinner et al., 2010; Waelbroeck et al., in press), which has a good resolution and is well dated. The simulated $\delta^{13}\text{C}_{ocean}$ at that site shows an increase of ~0.3 permil only (Figure 10 a), a small amplitude compared to the measured total variation of ~1.3 permil.

Atmospheric $\delta^{13}\text{C}_{atm}$ is sensitive to the evolution of the terrestrial biosphere (Figure

11 a). The difference between the simulated $\delta^{13}\text{C}_{atm}$ with fixed vegetation (“fixed veg”) and interactive vegetation gets greater with time and equals ~ 0.4 permil at -10,000 years. With fixed vegetation the changes in $\delta^{13}\text{C}_{atm}$ are only due to the ocean. As $\delta^{13}\text{C}_{ocean}$ does not change much it induces a constant $\delta^{13}\text{C}_{atm}$ value. The difference between the simulations with interactive vegetation and “fixed veg” is only due to the terrestrial biosphere whose **carbon content** progressively increases (Figure 8). Since the biosphere preferentially takes the light ^{12}C over ^{13}C during photosynthesis, the atmosphere becomes enriched in ^{13}C and $\delta^{13}\text{C}_{atm}$ increases (Figure 11 a). Yet, this trend disagrees with the data showing a “W” shape, suggesting a more complex evolution of mechanisms.

Even when taking carbonate compensation into account, the computed CO_2 , atmospheric and deep oceanic $\delta^{13}\text{C}$ evolutions are far from reproducing the evolution depicted by the data, underlining the need for additional mechanisms to explain the carbon cycle evolution. In the following, we test the three additional oceanic mechanisms described before during the deglaciation, and assess their impact on the carbon cycle evolution when the global climate warms.

3.2.2 Impact of iron fertilization

The simulated atmospheric CO_2 evolution improves when including the iron fertilization mechanism and rises from ~ 230 ppm at -21,000 years to ~ 260 ppm at -10,000 years (Figure 8 b). As the idealized experiment with a fixed climate has shown, the iron fertilization reacts quickly to the imposed forcing and the response thus follows the **iron** availability. The amplitude of the CO_2 change due to iron fertilization is probably overestimated in this simulation as a state-of-the-art GCM including an iron cycle indicates a more probable modern to LGM CO_2 decline of 15-20 ppm due to iron fertilization (Bopp et al., 2003; Tagliabue et al., 2009).

21

The computed LGM deep **ocean $\delta^{13}\text{C}$ evolution** also improves (Figure 10 b), yet its amplitude is clearly not large enough (the glacial value is ~ 0 permil compared to ~ -1 permil in the data). The $\delta^{13}\text{C}_{atm}$ evolution changes as well (Figure 11 b). The initial glacial value is increased by 0.2 permil compared to the control simulation. Following the evolution of **iron flux**, iron fertilization decreases during the deglaciation. Similarly to the terrestrial biosphere, marine biology preferentially uses ^{12}C over ^{13}C , which decreases $\delta^{13}\text{C}$ in the deep ocean and increases it in the upper ocean and atmosphere. When iron fertilization becomes lower, the biological pump decreases and the deep ocean **ocean $\delta^{13}\text{C}$** increases while $\delta^{13}\text{C}_{atm}$ decreases. In the atmosphere, because this effect is of the same amplitude as the effect of the terrestrial biosphere, but with an opposite sign, the overall simulated evolution of $\delta^{13}\text{C}_{atm}$ is flat.

3.2.3 Impact of the sinking of brines

Taking into account the halt of the sinking of brines improves the computed CO_2 evolution (Figure 8 c). Atmospheric CO_2 increases from ~ 220 ppm at -21,000 years to ~ 260 ppm at -10,000 years. The transition is however different for the two brine scenarios. When the sinking of brines is suddenly stopped (referred as “abrupt” in the Figure captions) the CO_2 rapidly increases. The degassing due to the break down of the stratification and reorganisation of the thermohaline circulation (Figure 12) takes approximately 3,000 years to reach the level of the control evolution. The linear reduction of the sinking of brines (“linear”) globally follows the forcing, which results in a smoother increase of atmospheric CO_2 . Yet, although the CO_2 evolution is slightly closer to the data when including the sinking of brines than with iron fertilization, none of them alone can account for the entire CO_2 rise during the deglaciation (Figure 8), which is mainly due to the mismatch of the initial states compared to the data.

The evolution of the deep **ocean $\delta^{13}\text{C}$** is improved compared to the control simulations (Figure 10 c) as the initial LGM $\delta^{13}\text{C}_{ocean}$ value is closer to the data (the simulated

$\delta^{13}\text{C}_{ocean}$ is ~ 0 permil compared to ~ 0.3 permil in the control simulations and ~ -1 permil in the data). It is nonetheless still too high compared to the data.

The sinking of brines has a more striking impact on $\delta^{13}\text{C}_{atm}$ (Figure 11 c). The abrupt halt of the sinking of brines at -18,000 years leads to a decrease of $\delta^{13}\text{C}_{atm}$ as the carbon from the deep ocean characterized by low $\delta^{13}\text{C}$ is released to the atmosphere. The decrease is larger when the vegetation is fixed because it only accounts for the oceanic change while in the simulation with interactive vegetation the increase of terrestrial biosphere **carbon content** (which increases $\delta^{13}\text{C}_{atm}$) counteracts the oceanic effect. When the halt of the sinking of brines is more progressive the change of $\delta^{13}\text{C}_{atm}$ due to the ocean takes place later so that when the vegetation is interactive the change due to the vegetation cancels out the one from the ocean and no decrease is simulated.

3.2.4 Impact of the sinking of brines and iron fertilization

With both the sinking of brines and iron fertilization included in the model, the entire amplitude of the CO_2 rise from ~ 190 ppm at -21,000 years to ~ 260 ppm at -10,000 years is simulated (Figure 8 d). The “abrupt” scenario leads to an early increase of CO_2 , which begins in advance compared to the data (**around 1000 years in advance**). The “linear” scenario is more similar to the data evolution. The separate effects of the sinking of brines and iron fertilization globally reinforce each other. Indeed, the sinking of brines alters the ocean dynamics while iron fertilization changes the marine biology. The sinking of brines induces a slight reduction of the surface nutrient concentration, hence a diminished effect of iron fertilization, yet the impact on atmospheric CO_2 is very small (a few ppm only). Thus the two mechanisms are almost independent of each other and their effects linearly add to each other. This combined effect is responsible for the very steep increase of CO_2 in the “abrupt” scenario as both mechanisms have a fast response of their own.

23

Yet the evolution of $\delta^{13}\text{C}_{ocean}$ is still far from the data (Figure 10 d), with a decrease of ~ 0.7 permil compared to ~ 1.3 permil in the data, mostly because of the mismatch between the initial value and the data. The sinking of brines has an important effect on $\delta^{13}\text{C}_{ocean}$ but the iron fertilization has a very small effect and the addition of the two cannot account for the entire measured evolution during the deglaciation.

The combination of the sinking of brines and iron fertilization yields better results for the $\delta^{13}\text{C}_{atm}$ evolution when the vegetation is fixed (Figure 11 d, dotted lines). In particular, between -18,000 years and -15,000 years the halt of the sinking of brines in addition to the diminishing iron fertilization produces a simulated $\delta^{13}\text{C}_{atm}$ decrease closer to the data. Yet when the vegetation is interactive (solid lines) this effect is counteracted by the increase of $\delta^{13}\text{C}_{atm}$ due to the expansion of the vegetation.

3.2.5 Impact of the sinking of brines and stratification-dependent diffusion

With a combination of the sinking of brines and the stratification-dependent diffusion, the amplitude of the CO_2 increase is also in line with the data (Figure 8 e). As observed with a constant climate forcing the effect of the brine induced stratification is amplified, the deep water mass is further isolated and stores more carbon at the LGM. The interactive diffusion also generates a delay in the oceanic response to the breakdown of the stratification and CO_2 is more progressively released. Hence the scenario that best agrees with the CO_2 record is now the “abrupt” scenario whereas the “linear” scenario is delayed and rises too late.

Contrary to the simulation with the sinking of brines and iron fertilization, the computed deep **ocean $\delta^{13}\text{C}$** is significantly improved (Figure 10 e) and the amplitude of the increase closer to the data. The interactive diffusion also amplifies the impact of the brines on $\delta^{13}\text{C}_{ocean}$, which is further decreased in the LGM and then increases to the Holocene value during the deglaciation. The scenario that best matches the data

24

evolution is again the “abrupt” scenario, the “linear” scenario yielding too late a rising.

However, the simulated $\delta^{13}\text{C}_{atm}$ does not really improve (Figure 11 e). It appears that the maxima of the “W” shape correspond to the values of the simulations with interactive vegetation while the minima are close to the values of the “fixed veg” simulations. Overall the $\delta^{13}\text{C}_{atm}$ record seems to oscillate between these two states, which could indicate a more complex evolution of the vegetation that a simple linear increase during the transition. The vegetation could begin to increase later than in the simulation, then decrease around -13,000 -12,000 years and then increase again (Köhler et al., 2005a). It confirms that the evolution of the terrestrial biosphere has an important impact on $\delta^{13}\text{C}_{atm}$ (Lourantou et al., 2010) and should be studied in more details in the future.

It results that the CO_2 evolution can be simulated in agreement with data either with the combination of brines and iron fertilisation or brines and interactive diffusion. However the evolution of $\delta^{13}\text{C}_{ocean}$ better match the data with the brine and interactive diffusion combination while the $\delta^{13}\text{C}_{atm}$ is slightly better with the brines and iron combination. In the following we thus take the three mechanisms simultaneously into account. Because the CO_2 is simulated in agreement with data we also change the version of the model to a fully carbon-climate coupled version. The simulations are thus not forced by a CO_2 record anymore.

3.3 Evolution of the mechanisms during the last deglaciation with interactive CO_2

Contrary to the previous section, here the climate and carbon models are fully coupled and atmospheric CO_2 is no longer prescribed but interactively computed. Because of this change in the version of the model, it is required to simulate new initial glacial conditions. We first evaluate these new glacial equilibrium runs before exploring the

25

evolution of the interactive carbon cycle during the deglaciation.

3.3.1 Initial glacial conditions

We first carry out two glacial equilibrium simulations with (“LGM-all”) and without (“LGM-ctrl”) the additional mechanisms studied. The runs start from previous glacial equilibrium runs (Bouttes et al., 2011) performed with prescribed CO_2 values (190 ppm) for the climate model. The values of the parameters for the additional mechanisms included in the “LGM-all” simulation are based on the results from ensemble simulations (Bouttes et al., 2011) ($frac=0.6$ for the sinking of brines, $iron=0.3$ for iron fertilization and $alpha=0.7$ for the stratification dependant diffusion). With these three additional mechanisms (“LGM-all”), the climate at the end of the 50,000 year simulation is slightly colder compared to the standard glacial simulation (0.3°C colder). The global air temperature during the LGM is 3.6°C colder compared to the preindustrial and the corresponding SST change is 2.3°C. In the “LGM-ctrl” run, CO_2 increases from ~254 ppm and equilibrates close to preindustrial level (~284 ppm) (Figure 13). The atmospheric CO_2 level is higher than the CO_2 prescribed due to the carbon-climate feedbacks. Indeed, higher CO_2 leads to higher temperature, which mainly reduces ocean solubility and further increases atmospheric CO_2 until it equilibrates. On the contrary, the “LGM-all” run is stable and the simulated CO_2 remains at the glacial level of ~190 ppm. Because of the deep stratification induced by the sinking of brines, the interactive diffusion and the iron fertilization, the deep ocean contains more carbon, hence the relatively low simulated CO_2 . Based on these mechanisms, because atmospheric CO_2 is now interactive, it is possible to study the temporal evolution of CO_2 during the deglaciation. Indeed, the ends of these equilibrium runs constitute the initial conditions for the deglacial runs.

3.3.2 Evolution of CO₂ and δ¹³C during the last deglaciation with a combination of mechanisms

As done previously, the ice sheet, sea level and insolation evolutions are prescribed. However, Atmospheric CO₂ is no longer prescribed but the one calculated by the carbon cycle module is used to compute the radiative scheme. The evolution of iron fertilization is again prescribed following **iron flux** data and different scenarios are applied to the brine mechanism (Figure 14a). The two scenarios explored before (linear decline “linear” and the sudden halt at 18ky BP “abrupt”) are again considered, and we also study two additional ones: a sudden halt of the sinking of brines at 17 ky BP “abrupt 17k” and an intermediate one “intermediate”.

In the control transient simulation (“CTRL”), atmospheric CO₂ roughly stays around 280 ppm (Figure 14b). This evolution is due to the terrestrial biosphere, whose **carbon content** increase lowers atmospheric CO₂. It counteracts the atmospheric CO₂ increase due to the rising temperatures causing lower solubility. This evolution widely differs from the data, i.e. a general increase from the glacial level of ~190 ppm until the Holocene value of ~260 ppm.

We then consider a combination of the three additional oceanic mechanisms during the deglaciation. With the combination of iron fertilization, sinking of brines and stratification dependent diffusion, the obtained computed transitions are mainly driven by the ocean and match the global data evolution of CO₂ better than the control simulation (Figure 14b). The scenarios that best match the data are the “abrupt 17k” and “intermediate” ones that support a relatively rapid halt of the sinking of brines when the Antarctic ice sheet is at its maximum extent. In these runs, the simulated deep Southern Ocean δ¹³C transition is also improved, with an increase of ~1 permil beginning at 15.5 kyr BP (Figure 14c). However, if the general trend is captured by the model, the CO₂ plateau during the Bolling-Allerod (from ~14 kyr BP to ~12 kyr BP) is not well

27

represented, underlining the lack of other processes such as abrupt AMOC variations that were not considered in this study.

This global behaviour for CO₂ and deep **ocean δ¹³C** during the termination is due to the modification of the ocean dynamics and reduced iron fertilization. The halt of the sinking of brines results in modifications of the overturning rate during the transition while iron fertilization induces changes in the biological production. During the glacial period, because of the sinking of brines, both the simulated North Atlantic Deep Water (NADW) and the Antarctic Bottom Water (AABW) export rates are weaker so that the deep water enriched in carbon is less mixed with the above water containing less carbon. As previously studied (Bouttes et al., 2010, 2011) the deep isolated water then represents an important carbon reservoir. The sinking of brines is responsible for a glacial CO₂ **change** of 39 ppm and the interactive diffusion scheme amplifies it by 16 ppm. During the transition the carbon trapped in the abyss is progressively released into the atmosphere because of the halt of the brines sink and break down of the stratification (Figure 15). In addition, the decrease in iron fertilization, which accounts for 10 ppm of the LGM CO₂ **change**, leads to a reduced biological production and therefore to a less effective biological pump. Similarly, the evolution of deep **ocean δ¹³C** is governed by the increasing mixing between surface water with high values of δ¹³C_{ocean} and deep water with low values of δ¹³C_{ocean}. Because of the change of oceanic circulation the deep values increase and the vertical gradient is diminished. **Although the general trend of the ocean δ¹³C evolution is well simulated with the model, the absolute values are slightly different. Because CLIMBER-2 is an intermediate complexity model with a low resolution and zonally averaged ocean, it complicates the comparison with the sediment core data. Similar experiments exploring the impacts of the sinking of brines with a better resolved 3D ocean model should lead to a better comparison.**

Although the amplitude of the glacial-interglacial Antarctic temperature change is underestimated in the model, it is possible to analyse the relative timing of CO₂ and

28

temperature evolution (Figure 16). The two scenarios that agree best with CO₂ and δ¹³C data (“abrupt 17k” and “intermediate”) result in a lead of temperature relative to CO₂ as inferred from termination 3 data (Caillon et al., 2003). The halt of the sinking of brines not only breaks down the stratification, which increases CO₂ and therefore temperature, but also induces a decrease in sea ice formation (which is computed by a thermodynamic sea ice model) as the surface waters become saltier and warmer. Such an early deglacial retreat of sea ice is also indicated in the data (Shemesh et al., 2002). Because of the reduced albedo, temperature then increases, resulting in a positive feedback. Antarctic temperature thus reacts quicker than CO₂ at the beginning of the termination, despite the same unique triggering, i.e. the halt of stratification due to brines sinking.

Recently, two papers studied the evolution of the carbon cycle in the context of glacial-interglacial cycles. Tschumi et al. (2011) run transient simulations testing the sensitivity of various mechanisms in a constant climate. The simulations support the hypothesis that a change in the ventilation of the deep ocean played an important role in the variation of CO₂ during glacial interglacial cycles. In this study, the change of deep ocean ventilation was obtained by changing the windstress whereas in our study the change of deep ocean stratification results from changing the sinking of brines. Our study also supports the important role of the change of deep ocean stratification. Furthermore it demonstrates that it allows to simulate the evolution of CO₂ during the last deglaciation in agreement with CO₂ and δ¹³C data without prescribing CO₂. In particular, the interactive carbon-climate simulation manages to capture not only the right CO₂ amplitude change, but also the right timing. With other mechanisms, Brovkin et al. (2011) run a full glacial-interglacial evolution of CO₂ and northern ice sheets. In this simulation the role of the carbonate compensation due to changes in the weathering rate is important. However, although most of the CO₂ evolution is successfully simulated, the timing of the CO₂ rise during the deglaciation lags the data indicating that a mechanism leading to an earlier CO₂ change is missing. With the change of

29

deep stratification from the change of sinking of brines it allows us to get this timing right, although it relies on scenarios that need to be confirmed.

4 Conclusions

To summarize, we use the intermediate complexity model CLIMBER-2 to explore the impact of three oceanic mechanisms on the evolution of the carbon cycle during the last deglaciation: iron fertilization, sinking of brines and stratification-dependent diffusion. The carbonate compensation mechanism is included in the CLIMBER-2 model, which has already been used to study the LGM carbon cycle (Brovkin et al., 2002b, 2007; Bouttes et al., 2009, 2010, 2011).

A first set of simulations in a context of a constant LGM climate has allowed an evaluation of the effect of each mechanism separately. The iron fertilization of marine biology induces the fastest response of the carbon cycle (~100 years) with a rapid increase in atmospheric CO₂ of ~29 ppm. The CO₂ rise due to the sinking of brines (~40 ppm) takes longer (almost 1,000 years) as it involves the oceanic circulation which takes more time to equilibrate than the marine biology. The combination of interactive diffusion with the sinking of brines induces an important delay as the vertical diffusion has to adjust to the evolving circulation. The carbon cycle then takes ~4,000 years to equilibrate. The impact of iron fertilization on δ¹³C_{ocean} is small (-0.12 permil). It is important for δ¹³C_{atm} (-0.25 permil). The effect of the sinking of brines is important on both deep ocean δ¹³C (-0.57 permil) and δ¹³C_{atm} (-0.25 permil). Adding the stratification-dependent diffusion amplifies the effect of the sinking of brines on CO₂ (61 ppm), deep ocean δ¹³C (-1.1 permil) and δ¹³C_{atm} (-0.34 permil) due to the decrease in mixing between the deep and upper waters, which makes the deep water enriched in carbon and depleted in δ¹³C even more isolated with more carbon and lower δ¹³C.

30

With the varying climate of the last termination the impact of the evolution of these mechanisms is modulated by other changes such as the warming and increase in the terrestrial biosphere **carbon content**. In this context, either the association of the sinking of brines with iron fertilization or with interactive diffusion results in a computed atmospheric CO₂ increase in agreement with the data. However, only the combination of brines with interactive diffusion also reconciles the simulated $\delta^{13}\text{C}_{\text{ocean}}$ with the recorded $\delta^{13}\text{C}$ evolution in the deep Southern Ocean. In the latter case, the scenario that best matches the data is the “abrupt” scenario, i.e. a sudden halt of the sinking of brines when the Antarctic ice sheet is at its maximum extent. In such a configuration sea ice formation is shifted to the open ocean instead of the shelf. The dense water from brine rejection is then mixed with fresher water preventing it to sink down to the abyss.

Based on the study of these mechanisms during the deglaciation and previous studies of the possible combinations of the mechanisms in glacial conditions (Bouttes et al., 2011), it is possible to use the model in an fully interactive carbon-climate version. The simulated evolution of CO₂ is in good agreement with the data underlining the powerful impact of the combination of the sinking of brines, stratification dependent diffusion and iron fertilization.

Although the computed CO₂ and deep **ocean $\delta^{13}\text{C}$** are in broad agreement with proxy data, the computed $\delta^{13}\text{C}_{\text{atm}}$ presents important discrepancies with respect to the data both in magnitude and structure. The persisting mismatch between model results and data for $\delta^{13}\text{C}_{\text{atm}}$ points to the role of vegetation, which could modulate the $\delta^{13}\text{C}_{\text{atm}}$ signal inducing low values when the vegetation is reduced and high values when the vegetation is increased. The change in the terrestrial biosphere seems to play a less important role for CO₂ and deep **ocean $\delta^{13}\text{C}$** , which are mostly driven by the oceanic mechanisms. This source discrimination between atmospheric mixing and isotopic CO₂ ratios has been recently explored (Lourantou et al., 2010). $\delta^{13}\text{C}_{\text{atm}}$ data can thus

31

help to constrain the vegetation evolution which is poorly known.

The $\delta^{13}\text{C}_{\text{atm}}$ mismatch can also point to the potential role of abrupt events, which were not considered in this study. Additionally, the lack of abrupt events is underlined by the absence of the CO₂ plateau during the Bolling-Allerod, as this plateau could also be linked to abrupt events associated to fresh water fluxes (Stocker and Wright, 1991). Indeed, fresh water fluxes, which can alter the thermohaline circulation, have an impact on the carbon cycle (Schmittner and Galbraith, 2008; Köhler et al., 2005b; Menviel et al., 2008b). Taking them into account could possibly improve both the CO₂ plateau and the $\delta^{13}\text{C}_{\text{atm}}$ evolution.

Acknowledgements. We thank Victor Brovkin, Andrey Ganopolski, Guy Munhoven and Emilie Capron for useful comments and discussion. We also thank the editor and two anonymous reviewers for their comments which helped improve this manuscript.

References

- Archer, D.: Modeling the Calcite Lysocline, *J. Geophys. Res.*, 96(C9), 17,037–17,050, 1991.
- Archer, D., Winguth, A., Lea, D., and Mahowald, N.: What caused the glacial / interglacial pCO₂ cycles?, *Rev. Geophys.*, 38, 159–189, 2000.
- Archer, D. E., Martin, P. A., Milovich, J., Brovkin, V., Plattner, G.-K., and Ashendel, C.: Model sensitivity in the effect of Antarctic sea ice and stratification on atmospheric pCO₂, *Paleoceanography*, 18(1), 1012, doi:10.1029/2002PA000760, 2003.
- Barker, S., Diz, P., Vautravers, M. J., Pike, J., Knorr, G., Hall, I. R., and Broecker, W. S.: Interhemispheric Atlantic seesaw response during the last deglaciation, *Nature*, 457, 1097–1102, doi:10.1038/nature07770, 2009.
- Berger, A., Loutre, M. F., and Galle, H.: Sensitivity of the LLN climate model to the astronomical and CO₂ forcings over the last 200 ky, *Climate Dyn.*, 14 (9), 615–629, doi: 10.1007/s003820050245, 1998.
- Berger, A. L.: Long-term variations of daily insolation and Quaternary climatic changes, *J. Atmos. Sci.*, 35, 2362–2368, 1978.

32

- Berger, W. H.: Increase of carbon dioxide in the atmosphere during Deglaciation: the coral reef hypothesis, *Naturwissenschaften*, 69, 87–88, 1982.
- Bird, M. I., Lloyd, J., and Farquhar, G. D.: Terrestrial carbon storage at the LGM, *Nature*, 371, 566, 1994.
- Bopp, L., Kohfeld, K. E., Quéré, C. L., and Aumont, O.: Dust impact on marine biota and atmospheric CO₂ during glacial periods, *Paleoceanography*, 18(2), 1046, doi:10.1029/2002PA000810, 2003.
- Bouttes, N., Roche, D. M., and Paillard, D.: Impact of strong deep ocean stratification on the carbon cycle, *Paleoceanography*, 24, PA3203, doi:10.1029/2008PA001707, 2009.
- Bouttes, N., Paillard, D., and Roche, D. M.: Impact of brine-induced stratification on the glacial carbon cycle, *Clim. Past*, 6, 575–589, doi:10.5194/cpd-6-681-2010, 2010.
- Bouttes, N., Paillard, D., Roche, D. M., Brovkin, V., and Bopp, L.: Last Glacial Maximum CO₂ and $\delta^{13}\text{C}$ successfully reconciled, *Geophys. Res. Lett.*, 38, L02705, doi:10.1029/2010GL044499, 2011.
- Broecker, W. S. and Peng, T.-H., eds.: *Tracers in the Sea*, Lamont-Doherty Geological Observatory of Columbia University, Palisades, New York, 1982.
- Broecker, W. S. and Peng, T.-H.: The Role of CaCO₃ Compensation in the Glacial to Interglacial Atmospheric CO₂ Change, *Global Biogeochem. Cycles*, 1(1), 15–29, 1987.
- Brovkin, V., Bendtsen, J., Claussen, M., Ganopolski, A., Kubatzki, C., Petoukhov, V., and Andreev, A.: Carbon cycle, vegetation, and climate dynamics in the Holocene: Experiments with the CLIMBER-2 model, *Global Biogeochem. Cycles*, 16(4), 1139, doi:10.1029/2001GB001662, 2002a.
- Brovkin, V., Hofmann, M., Bendtsen, J., and Ganopolski, A.: Ocean biology could control atmospheric $\delta^{13}\text{C}$ during glacial-interglacial cycle, *Geochem. Geophys. Geosyst.*, 3(5), 1027, doi:10.1029/2001GC000270, 2002b.
- Brovkin, V., Ganopolski, A., Archer, D., and Rahmstorf, S.: Lowering of glacial atmospheric CO₂ in response to changes in oceanic circulation and marine biogeochemistry, *Paleoceanography*, 22, PA4202, doi:10.1029/2006PA001380, 2007.
- Brovkin, V., Ganopolski, A., Archer, D., and Munhoven, G.: Glacial CO₂ cycle as a succession of key physical and biogeochemical processes, *Clim. Past Discuss.*, 7, 1767–1795, doi:10.5194/cpd-7-1767-2011, 2011.
- Caillon, N., Severinghaus, J. P., Jouzel, J., Barnola, J.-M., Kang, J., and Lipenkov, V. Y.: Timing of Atmospheric CO₂ and Antarctic Temperature Changes Across Termination III, *Science*,

33

- 299, 1728, doi:10.1126/science.1078758, 2003.
- Charbit, S., Kageyama, M., Roche, D., Ritz, C., and Ramstein, G.: Investigating the mechanisms leading to the deglaciation of past continental northern hemisphere ice sheets with the CLIMBER GREMLINS coupled model, *Global Planet. Change*, 48, 253–273, doi:10.1016/j.gloplacha.2005.01.002, 2005.
- Clark, P. U., Dyke, A. S., Shakun, J. D., Carlson, A. E., Clark, J., Wohlfarth, B., Mitrovica, J. X., Hostetler, S. W., and McCabe, A. M.: The Last Glacial Maximum, *Science*, 325, 710–714, doi:10.1126/science.1172873, 2009.
- Crowley, T.: Ice Age Terrestrial Carbon Changes Revisited, *Global Biogeochem. Cycles*, 9(3), 377–389, 1995.
- Cuffey, K. M. and Vimeux, F.: Covariation of carbon dioxide and temperature from the Vostok ice core after deuterium-excess correction, *Nature*, 412, 523–527, doi:10.1038/35087544, 2001.
- Curry, W. B. and Oppo, D. W.: Glacial water mass geometry and the distribution of $\delta^{13}\text{C}$ of ΣCO_2 in the western Atlantic Ocean, *Paleoceanography*, 20, PA1017, doi:10.1029/2004PA001021, 2005.
- EPICA community members: Eight glacial cycles from an Antarctic ice core, *Nature*, 429, 623–628, 2004.
- Fischer, H., Schmitt, J., Lüthi, D., Stocker, T. F., Tschumi, T., Parekh, P., Joos, F., Köhler, P., Völker, C., Gersonde, R., Barbante, C., Floch, M. L., Raynaud, D., and Wolff, E.: The role of Southern Ocean processes on orbital and millennial CO₂ variations - a synthesis, *Quat. Sci. Rev.*, 29 (1-2), 193–205, doi:10.1016/j.quascirev.2009.06.007, 2010.
- Ganopolski, A. and Rahmstorf, S.: Rapid changes of glacial climate simulated in a coupled climate model, *Nature*, 409, 153–158, 2001.
- Ganopolski, A., Petoukhov, V., Rahmstorf, S., Brovkin, V., Claussen, M., Eliseev, A., and Kubatzki, C.: CLIMBER-2: A climate system model of intermediate complexity, part II: Model sensitivity, *Clim. Dyn.*, 17, 735–751, 2001.
- Ganopolski, A., Calov, R., and Claussen, M.: Simulation of the last glacial cycle with a coupled climate ice-sheet model of intermediate complexity, *Clim. Past*, 6, 229–244, doi:10.5194/cp-6-229-2010, 2010.
- Gersonde, R., Crosta, X., Abelmann, A., and Armand, L.: Sea-surface temperature and sea ice distribution of the Southern Ocean at the EPILOG Last Glacial Maximum - a circum-Antarctic view based on siliceous microfossil records, *Quat. Sci. Rev.*, 24, 869–896, 2005.
- Hodell, D. A., Venz, K. A., Charles, C. D., and Ninnemann, U. S.: Pleistocene vertical car-

34

- bon isotope and carbonate gradients in the South Atlantic sector of the Southern Ocean, *Geochem. Geophys. Geosyst.*, 4 (1), 1–19, doi:10.1029/2002GC000367, 2003.
- Huybrechts, P.: Sea-level changes at the LGM from ice-dynamic reconstructions of the Greenland and Antarctic ice sheets during the glacial cycles, *Quat. Sci. Rev.*, 21 (1-3), 203–231, doi:10.1016/S0277-3791(01)00082-8, 2002.
- Jouzel, J., Masson-Delmotte, V., Cattani, O., Dreyfus, G., Falourd, S., Hoffmann, G., Minster, B., Nouet, J., Barnola, J. M., Chappellaz, J., Fischer, H., Gallet, J. C., Johnsen, S., Leuenberger, M., Loulergue, L., Luethi, D., Oerter, H., Parrenin, F., Raisbeck, G., Raynaud, D., Schilt, A., Schwander, J., Selmo, E., Souchez, R., Spahni, R., Stauffer, B., Steffensen, J. P., Stenni, B., Stocker, T. F., Tison, J. L., Werner, M., and Wolf, E. W.: Orbital and Millennial Antarctic Climate Variability over the Past 800,000 Years, *Science*, 317, 793, doi:10.1126/science.1141038, 2007.
- Kaplan, J. O., Prentice, I. C., Knorr, W., and Valdes, P. J.: Modeling the dynamics of terrestrial carbon storage since the Last Glacial Maximum, *Geophys. Res. Lett.*, 29(22), 2074, doi:10.1029/2002GL015230, 2002.
- Keigwin, L. D., Jones, G. A., Lehman, S. J., and Boyle, E. A.: Deglacial Meltwater Discharge, North Atlantic Deep Circulation, and Abrupt Climate Change, *J. Geophys. Res.*, 96(C9), 16,811 – 16,826, 1991.
- Kohfeld, K. E., Quéré, C. L., Harrison, S. P., and Anderson, R. F.: Role of Marine Biology in Glacial-Interglacial CO₂ Cycles, *Science*, 308, 74–78, 2005.
- Köhler, P. and Fischer, H.: Simulating changes in the terrestrial biosphere during the last glacial/interglacial transition, *Global Planet. Change*, 43, 33–55, doi:10.1016/j.globalcha.2004.02.005, 2004.
- Köhler, P., Fischer, H., Munhoven, G., and Zeebe, R. E.: Quantitative interpretation of atmospheric carbon records over the last glacial termination, *Global Biogeochem. Cycles*, 19, GB4020, doi:10.1029/2004GB002345, 2005a.
- Köhler, P., Joos, F., Gerber, S., and Knutti, R.: Simulated changes in vegetation distribution, land carbon storage, and atmospheric CO₂ in response to a collapse of the North Atlantic thermohaline circulation, *Climate Dyn.*, 25, 689–708, doi:10.1007/s00382-005-0058-8, 2005b.
- Lourantou, A., Lavric, J. V., Köhler, P., Barnola, J.-M., Paillard, D., Michel, E., Raynaud, D., and Chappellaz, J.: Constraint of the CO₂ rise by new atmospheric carbon isotopic measurements during the last deglaciation, *Global Biogeochem. Cycles*, 24, GB2015, doi:10.1029/2009GB003545, 2010.

35

- Mackintosh, A., Golledge, N., Domack, E., Dunbar, R., Leventer, A., White, D., Pollard, D., DeConto, R., Fink, D., Zwart, D., Gore, D., and Lavoie, C.: Retreat of the East Antarctic ice sheet during the last glacial termination, *Nature geoscience*, 4, 195–202, doi:10.1038/ngeo1061, 2011.
- MARGO Project Members: Constraints on the magnitude and patterns of ocean cooling at the Last Glacial Maximum, *Nature Geosci.*, 2, 127–132, doi:10.1038/ngeo411, 2009.
- Martin, J. H.: Glacial-Interglacial CO₂ change: the iron hypothesis, *Paleoceanography*, 5, 1–13, 1990.
- Marzeion, B., Levermann, A., and Mignot, J.: The Role of Stratification-Dependent Mixing for the Stability of the Atlantic Overturning in a Global Climate Model, *J. Phys. Oceanogr.*, 37, 2672–2681, doi:10.1175/2007JPO3641.1, 2007.
- Menviel, L., Timmermann, A., Mouchet, A., and Timm, O.: Climate and marine carbon cycle response to changes in the strength of the Southern Hemispheric westerlies, *Paleoceanography*, 23, PA4201, doi:10.1029/2008PA001604, 2008a.
- Menviel, L., Timmermann, A., Mouchet, A., and Timm, O.: Meridional reorganizations of marine and terrestrial productivity during Heinrich events, *Paleoceanography*, 23, PA1203, doi:10.1029/2007PA001445, 2008b.
- Monnin, E., Indermühle, A., Daellenbach, A., Flueckiger, J., Stauffer, B., Stocker, T. F., Raynaud, D., and Barnola, J.-M.: Atmospheric CO₂ concentrations over the Last Glacial Termination, *Science*, 291, 112–114, 2001.
- Montenegro, A., Eby, M., Kaplan, J. O., Meissner, J., and Weaver, A. J.: Carbon storage on exposed continental shelves during the glacial-interglacial transition, *Geophys. Res. Lett.*, 33, L08 703, doi:10.1029/2005GL025480, 2006.
- North Greenland Ice Core Project members: High-resolution record of Northern Hemisphere climate extending into the last interglacial period, *Nature*, 431, 147–151, doi:10.1038/nature02805, 2004.
- Opdyke, B. N. and Walker, J. C. G.: Return of the coral reef hypothesis: Basin to shelf partitioning of CaCO₃ and its effect on atmospheric CO₂, *Geology*, 20, 733–736, 1992.
- Paillard, D. and Parrenin, F.: The Antarctic ice sheet and the triggering of deglaciations, *Earth Planet. Sci. Lett.*, 227, 263–271, 2004.
- Peltier, W. R.: Ice age paleotopography, *Science*, 265, 195–201, doi:10.1126/science.265.5169.195, 1994.
- Peltier, W. R.: Global glacial isostasy and the surface of the ice-age Earth: The ICE-5G (VM2)

36

- Model and GRACE, *Annu. Rev. Earth Planet. Sci.*, 32, 111–49, doi:10.1146/annurev.earth.32.082503.144359, 2004.
- Petoukhov, V., Ganopolski, A., Eliseev, A., Kubatzki, C., and Rahmstorf, S.: CLIMBER-2: A climate system model of intermediate complexity, part I: Model description and performance for present climate, *Clim. Dyn.*, 16, 1–17, 2000.
- Ritz, C., Rommelaere, V., and Dumas, C.: Modeling the evolution of Antarctic ice sheet over the last 420,000 years: Implications for altitude changes in the Vostok region, *J. Geophys. Res.*, 106, 31,943–31,964, 2001.
- Schmittner, A. and Galbraith, E. D.: Glacial greenhouse-gas fluctuations controlled by ocean circulation changes, *Nature*, 456, 373–376, doi:10.1038/nature07531, 2008.
- Shemesh, A., Hodell, D., Crosta, X., Kanfoush, S., Charles, C., and Guilderson, T.: Sequence of events during the last deglaciation in Southern Ocean sediments and Antarctic ice cores, *Paleoceanography*, 17 (4), 1056, doi:10.1029/2000PA000599, 2002.
- Sigman, D. M. and Boyle, E. A.: Glacial/interglacial variations in atmospheric carbon dioxide, *Nature*, 407, 859–869, doi:10.1038/35038000, 2000.
- Sigman, D. M., Hain, M. P., and Haug, G. H.: The polar ocean and glacial cycles in atmospheric CO₂ concentration, *Nature*, 466, 47–55, doi:10.1038/nature09149, 2010.
- Skinner, L. C., Fallon, S., Waelbroeck, C., Michel, E., and Barker, S.: Ventilation of the Deep Southern Ocean and Deglacial CO₂ Rise, *Science*, 328 (5982), 1147–1151, doi:10.1126/science.1183627, 2010.
- Stephens, B. B. and Keeling, R. F.: The influence of Antarctic sea ice on glacial-interglacial CO₂ variations, *Nature*, 404, 171–174, 2000.
- Stocker, T. F. and Wright, D.: Rapid transitions of the ocean's deep circulation induced by changes in the surface water fluxes, *Nature*, 351, 729–732, 1991.
- Svendsen, J. I., Alexanderson, H., Astakhov, V. I., Demidov, I., Dowdeswell, J. A., Funder, S., Gataullin, V., Henriksen, M., Hjort, C., Houmark-Nielsen, M., Hubberten, H. W., Ingfsson, J., Jakobsson, M., Kjr, K. H., Larsen, E., Lokrantz, H., Lunkka, J. P., Lys, A., Mangerud, J., Matiouchkov, A., and et al.: Late Quaternary ice sheet history of northern Eurasia, *Quat. Sci. Rev.*, 23 (11-13), 1229–1271, doi:10.1016/j.quascirev.2003.12.008, 2004.
- Tagliabue, A., Bopp, L., Roche, D. M., Bouttes, N., Dutay, J.-C., Alkama, R., Kageyama, M., Michel, E., and Paillard, D.: Quantifying the roles of ocean circulation and biogeochemistry in governing ocean carbon-13 and atmospheric carbon dioxide at the last glacial maximum, *Clim. Past*, 5, 695–706, 2009.

- Toggweiler, J. R.: Variation of atmospheric CO₂ by ventilation of the ocean's deepest water, *Paleoceanography*, 14(5), 571–588, 1999.
- Toggweiler, J. R., Russell, J. L., and Carson, S. R.: Midlatitude westerlies, atmospheric CO₂, and climate change during the ice ages, *Paleoceanography*, 21, PA2005, doi:10.1029/2005PA001154, 2006.
- Tschumi, T., Joos, F., Gehlen, M., and Heinze, C.: Deep ocean ventilation, carbon isotopes, marine sedimentation and the deglacial CO₂ rise, *Clim. Past*, 7, 771–800, doi:10.5194/cp-7-771-2011, 2011.
- Visser, K., Thunell, R., and Stott, L.: Magnitude and timing of temperature change in the Indo-Pacific warm pool during deglaciation, *Nature*, 421, 152–155, doi:10.1038/nature01297, 2003.
- von Deimling, T. S., Ganopolski, A., Held, H., and Rahmstorf, S.: How cold was the Last Glacial Maximum?, *Geophys. Res. Lett.*, 33, L14 709, doi:10.1029/2006GL026484, 2006.
- Waelbroeck, C., Labeyrie, L., Michel, E., Duplessy, J. C., McManus, J. F., Lambeck, K., Balbon, E., and Labracherie, M.: Sea-level and deep water temperature changes derived from benthic foraminifera isotopic records, *Quat. Sci. Rev.*, 21(1-3), 295–305, doi:10.1016/S0277-3791(01)00101-9, 2002.
- Waelbroeck, C., Skinner, L. C., Labeyrie, L., Duplessy, J.-C., Michel, E., Riveiros, N. V., Gherardi, J.-M., and Dewilde, F.: The timing of deglacial circulation changes in the Atlantic, *Paleoceanography*, doi:10.1029/2010PA002007, in press.
- Watson, A. J. and Garabato, A. C. N.: The role of Southern Ocean mixing and upwelling in glacial-interglacial atmospheric CO₂ change, *Tellus B*, 58 (1), 73–87, doi:10.1111/j.1600-0889.2005.00167.x, 2005.
- Wolff, E. W., Fischer, H., Fundel, F., Ruth, U., Twarloh, B., Littot, G. C., Mulvaney, R., Rthlisberger, R., de Angelis, M., Boutron, C. F., Hansson, M., Jonsell, U., Hutterli, M. A., Lambert, F., Kaufmann, P., Stauffer, B., Stocker, T. F., Steffensen, J. P., Bigler, M., Siggaard-Andersen, M. L., Udisti, R., Becagli, S., Castellano, E., Severi, M., Wagenbach, D., Barbante, C., Gabrielli, P., and Gaspari, V.: Southern Ocean sea-ice extent, productivity and iron flux over the past eight glacial cycles, *Nature*, 440, 491–496, doi:10.1038/nature04614, 2006.

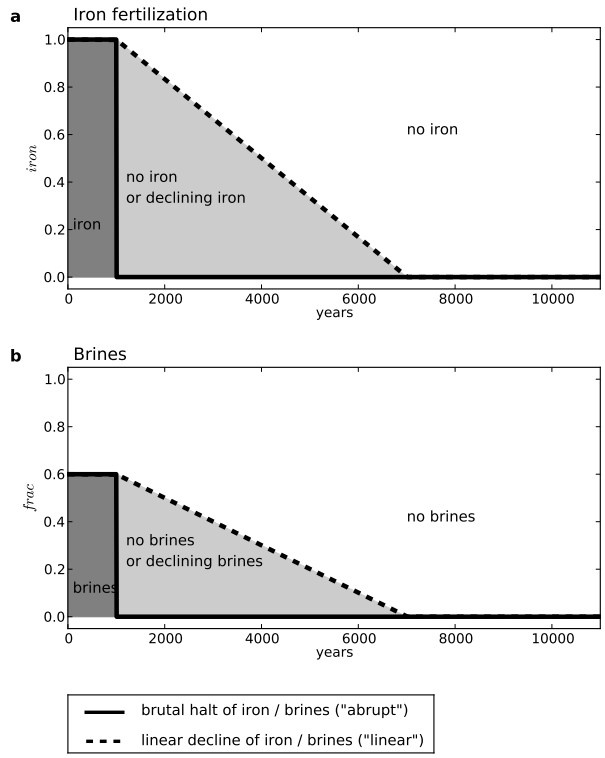


Fig. 1. Evolution scenarios for iron fertilization and the sinking of brines with a constant climate. The two processes are active at the beginning of the simulations then stop. This stop can be sudden or follow a linear decline.

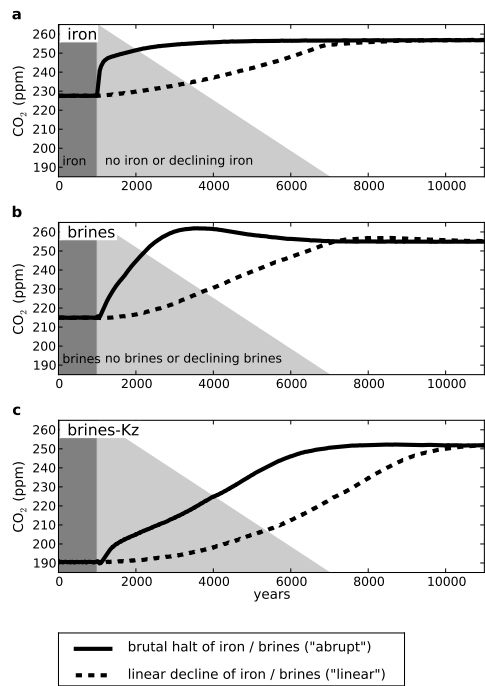


Fig. 2. Evolution of atmospheric CO₂ with a constant climate for three mechanisms: (a) iron fertilization, (b) sinking of brines and (c) sinking of brines and interactive vertical diffusion.

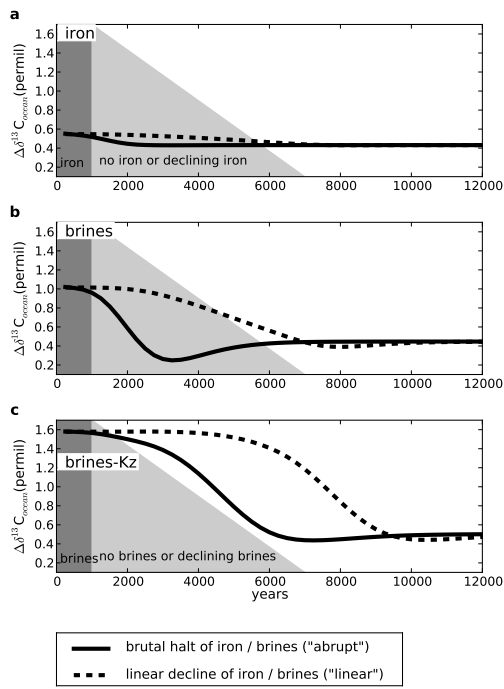


Fig. 3. Evolution of oceanic $\Delta\delta^{13}C_{ocean}$ with a constant climate for three mechanisms: (a) iron fertilization, (b) sinking of brines and (c) sinking of brines and interactive vertical diffusion.

41

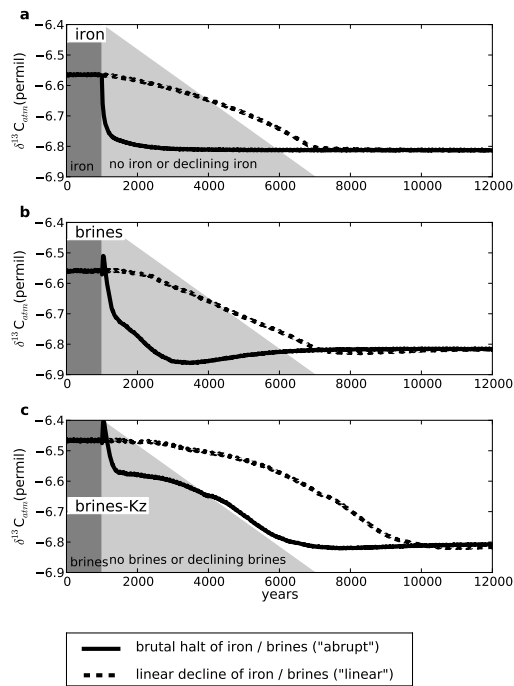


Fig. 4. Evolution of atmospheric $\delta^{13}C_{atm}$ with a constant climate for three mechanisms: (a) iron fertilization, (b) sinking of brines and (c) sinking of brines and interactive vertical diffusion.

42

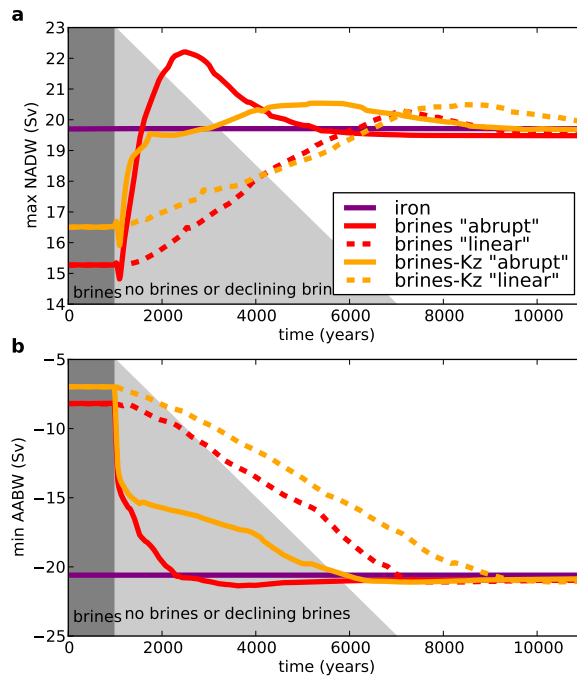


Fig. 5. Evolution of the thermohaline circulation with a constant climate. (a) Evolution of the maximum value of the North Atlantic stream function (Sv) and (b) evolution of the minimum value of the Southern Ocean stream function (Sv).

43

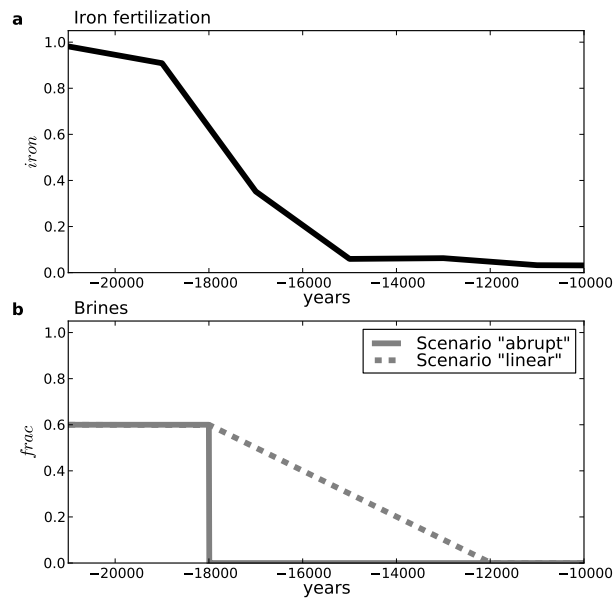


Fig. 6. Evolution scenarios for (a) iron fertilization and (b) the sinking of brines during the last deglaciation. The two processes are active at the beginning of the simulations then stop. The iron fertilization decline follows the dust transport as recorded in ice cores (Wolff et al., 2006). The halt of the sinking of brines follows two scenarios: a sudden halt ("abrupt") or a linear decline ("linear").

44

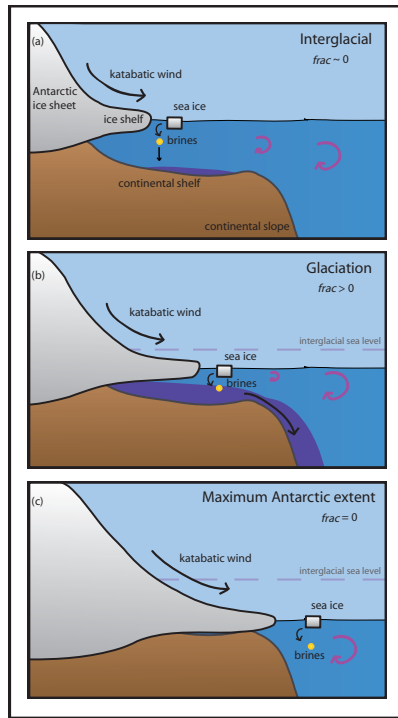


Fig. 7. Schematic representation of the sinking of brines during (a) interglacial, (b) glacial and (c) deglacial periods. The main drivers of the fraction of salt sinking to the deep ocean ($frac$) are the Antarctic ice sheet extent on the continental shelf and sea level which govern the volume of water above the continental shelf. The less water there is the less brines are mixed and the more they can sink to the deep ocean. When sea ice formation is shifted to the open ocean brines are mixed and the sinking stops.

45

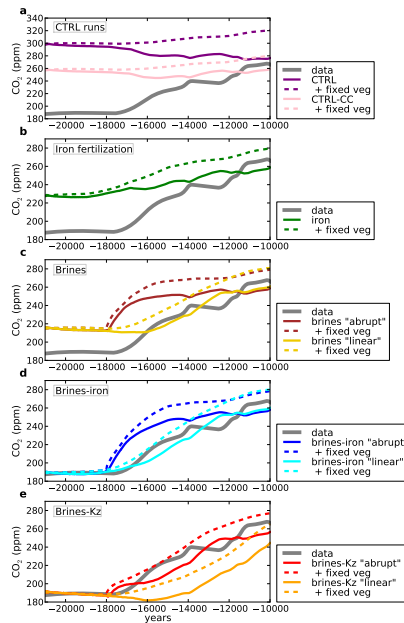


Fig. 8. Evolution of atmospheric CO_2 during the last deglaciation with different oceanic mechanisms and comparison with data: (a) control (CTRL) runs without and with carbonate compensation (CC), all other simulations are with carbonate compensation, (b) simulations with iron fertilization, (c) simulations with the sinking of brines (two scenarios as defined in Figure 6), (d) simulations with the sinking of brines (two scenarios as defined in Figure 6) and iron fertilization, (e) simulations with the sinking of brines (two scenarios as defined in Figure 6) and interactive vertical diffusion coefficient (Kz). Each simulation has either an interactive vegetation or a fixed glacial vegetation ("fixed veg"). The data are from Monnin et al. (2001); Lourantou et al. (2010).

46

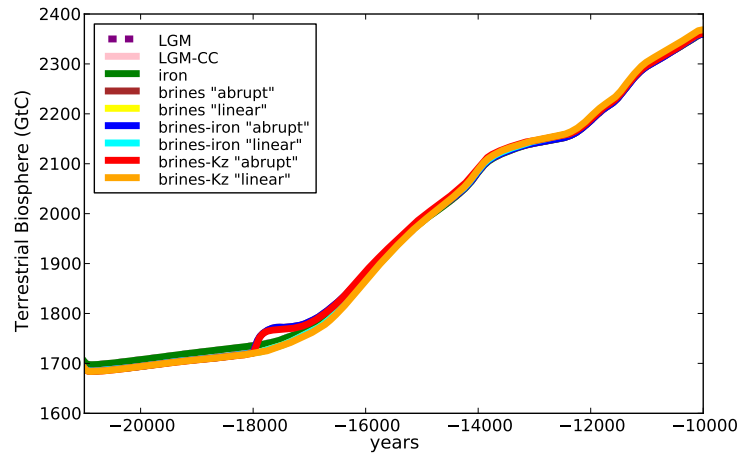


Fig. 9. Evolution of the carbon stock from the terrestrial biosphere (GtC) during the deglaciation for the simulations as defined in figures 7, 8 and 9, when the terrestrial biosphere is interactive.

47

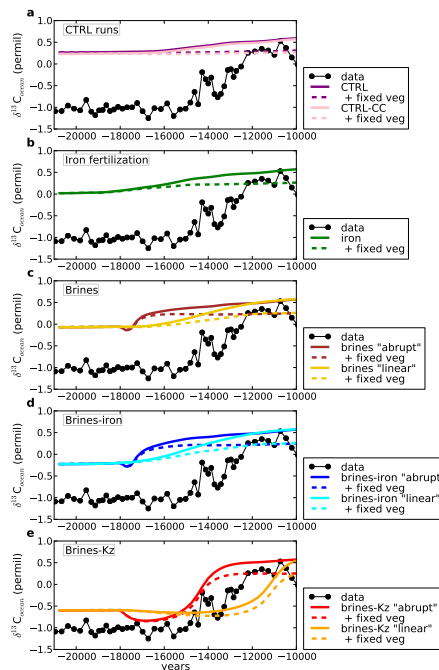


Fig. 10. Evolution of deep Southern Ocean $\delta^{13}\text{C}$ during the last deglaciation with different oceanic mechanisms and comparison with data: (a) control (CTRL) runs without and with carbonate compensation (CC), all other simulations are with carbonate compensation, (b) simulations with iron fertilization, (c) simulations with the sinking of brines (two scenarios as defined in Figure 6), (d) simulations with the sinking of brines (two scenarios as defined in Figure 6) and iron fertilization, (e) simulations with the sinking of brines (two scenarios as defined in Figure 6) and interactive vertical diffusion coefficient (K_z). Each simulation has either an interactive vegetation or a fixed glacial vegetation (“fixed veg”). The data are from Waelbroeck et al. (in press). The localisation of the core (MD07-3076Q) is 44°S, 14°W, 3770m.

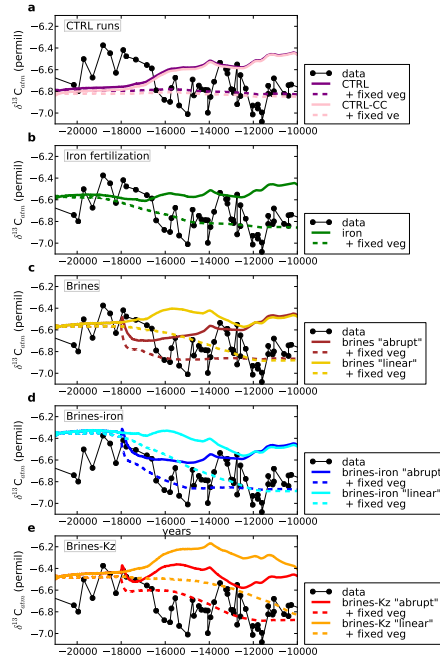


Fig. 11. Evolution of atmospheric $\delta^{13}C_{atm}$ during the last deglaciation with different oceanic mechanisms and comparison with data: (a) control (CTRL) runs without and with carbonate compensation (CC), all other simulations are with carbonate compensation, (b) simulations with iron fertilization, (c) simulations with the sinking of brines (two scenarios as defined in Figure 6), (d) simulations with the sinking of brines (two scenarios as defined in Figure 6) and iron fertilization, (e) simulations with the sinking of brines (two scenarios as defined in Figure 6) and interactive vertical diffusion coefficient (K_z). Each simulation has either an interactive vegetation or a fixed glacial vegetation ("fixed veg"). The data are from Lourantou et al. (2010).

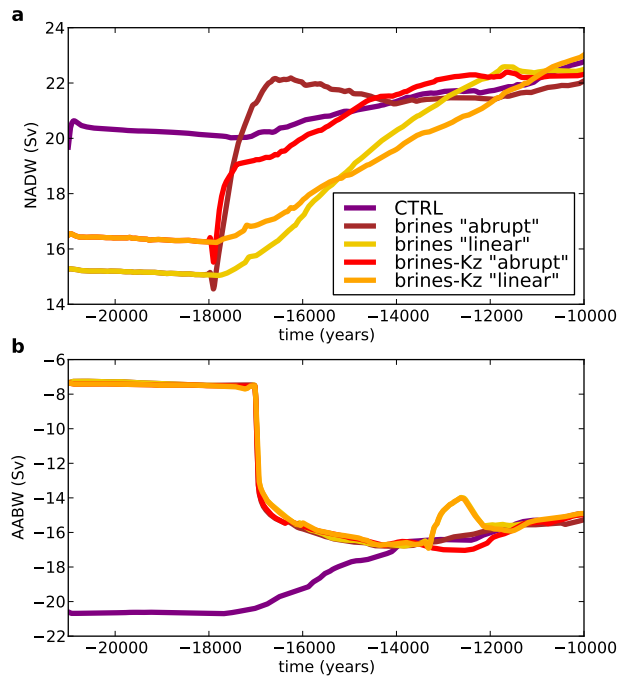


Fig. 12. Evolution of the thermohaline circulation during the deglaciation. (a) Evolution of the maximum value of the North Atlantic stream function (Sv) and (b) evolution of the maximum value of the Southern Ocean stream function (Sv). The sign denotes the circulation direction which is positive from south to north.

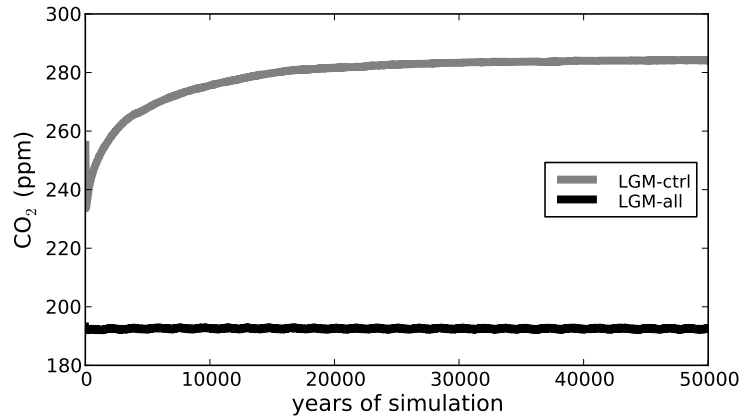


Fig. 13. Equilibrium simulations with LGM boundary conditions (LGM ice sheets and orbital parameters) with carbonate compensation (“LGM-ctrl”) and with the combination of the three additional mechanisms (“LGM-all”, sinking of brines, interactive diffusion and iron fertilization).

51

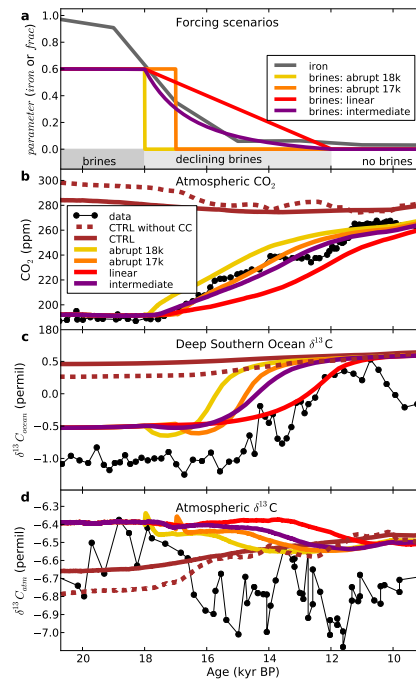


Fig. 14. Forcing scenarios and simulated evolution of atmospheric CO_2 , deep Southern Ocean $\delta^{13}\text{C}$ and atmospheric $\delta^{13}\text{C}$ during the deglaciation. (a) Evolution scenarios for the iron fertilization (*iron* parameter, grey) and sinking of brines (*frac* parameter, colors), (b) simulated evolution of atmospheric CO_2 (ppm) for the control run (“CTRL” in brown, without carbonate compensation: dotted line and with carbonate compensation: solid line) and with three additional mechanisms: interactive diffusion, iron fertilization and different brine scenarios as described in figure 14a compared to data (black circles), (c) evolution of deep Southern Ocean $\delta^{13}\text{C}$ (permil) for the same simulations and (d) of atmospheric $\delta^{13}\text{C}$ (permil).

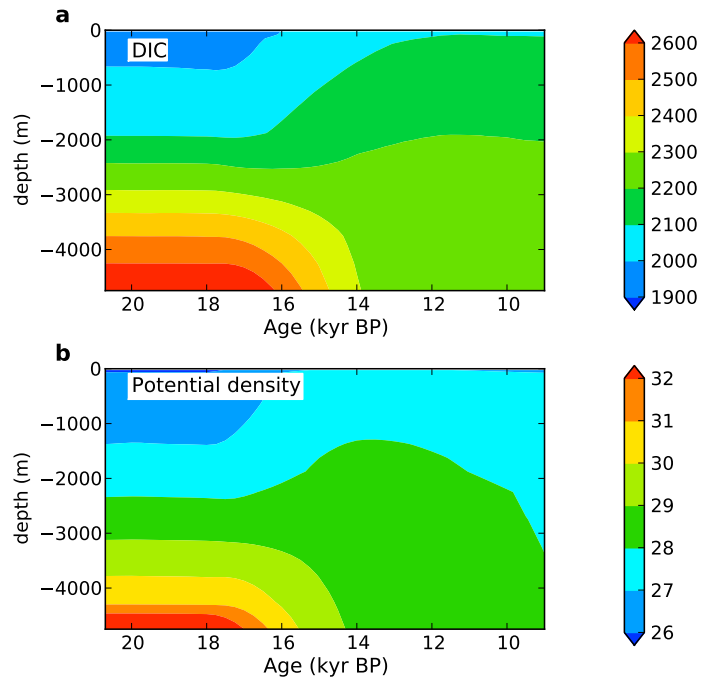


Fig. 15. Evolution of (a) Dissolved Inorganic Carbon (DIC, $\mu\text{mol kg}^{-1}$) and (b) potential density anomaly ($\rho_{\theta} - 1,000 \text{ kg m}^{-3}$) as a function of depth at latitude 50°S of the Atlantic ocean sector.

53

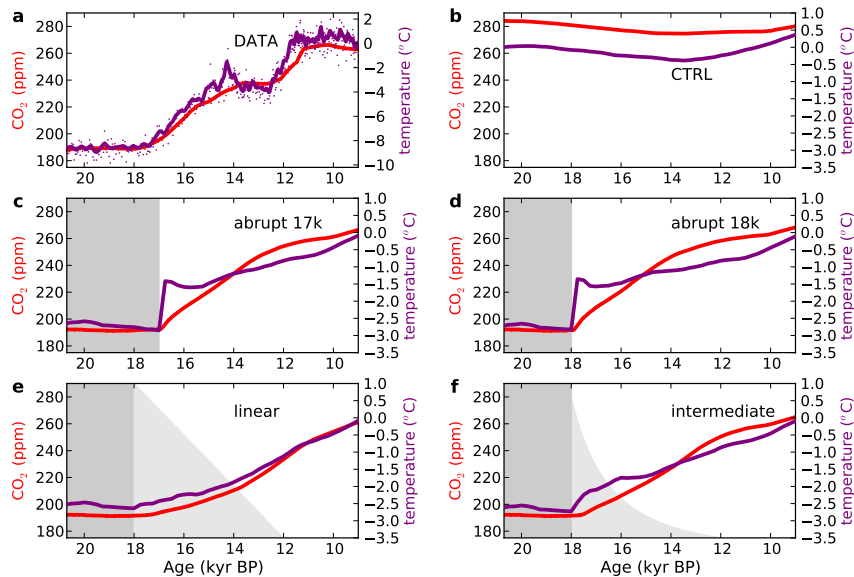


Fig. 16. Timing of CO_2 (ppm) and Antarctic temperature ($^{\circ}\text{C}$) evolution during the deglaciations for (a) the data (Monnin et al., 2001; Lourantou et al., 2010; Jouzel et al., 2007), (b) the CTRL simulation (with carbonate compensation), (c, d, e and f) the simulations with interactive diffusion, iron fertilization and different brines scenarios as defined in figure 14a. The grey shading indicates the evolution of the sinking of brines according to each scenario.

54

	CO ₂ (ppm)	$\Delta\delta^{13}\text{C}_{ocean}$ (permil)	$\delta^{13}\text{C}_{atm}$ (permil)
Iron	29	-0.12	-0.25
Brines	40	-0.57	-0.25
Brines-K _z	61	-1.1	-0.34

Table 1. Amplitude of change between the beginning and the end of the simulations under a constant glacial climate as observed on figures 2, 3 and 4. *Iron* corresponds to iron fertilization, *Brines* to the sinking of brines and *Brines-K_z* to the sinking of brines and interactive diffusion.

a) CO₂

	"abrupt" scenario	"linear" scenario
Iron	120 years	4360 years
Brines	900 years	4370 years
Brines-K _z	4270 years	7440 years

b) $\Delta\delta^{13}\text{C}_{ocean}$

	"abrupt" scenario	"linear" scenario
Iron	1250 years	6250 years
Brines	1250 years	5750 years
Brines-K _z	5000 years	8250 years

c) $\delta^{13}\text{C}_{atm}$

	"abrupt" scenario	"linear" scenario
Iron	1270 years	5890 years
Brines	1270 years	5850 years
Brines-K _z	5140 years	8570 years

Table 2. Time for the anomaly of the considered variable (defined as the difference between its value and the initial value) to reach 95% of the equilibrium anomaly value (equilibrium anomaly value taken as the difference between the value at year 12000 of the simulations and the initial value) under a constant glacial climate for (a) CO₂, (b) $\Delta\delta^{13}\text{C}_{ocean}$ and (c) $\delta^{13}\text{C}_{atm}$. *Iron* corresponds to iron fertilization, *Brines* to the sinking of brines and *Brines-K_z* to the sinking of brines and interactive diffusion. The two scenarios for iron fertilization and the sinking of brines ("abrupt" and "linear") are defined in figure 1.